

Article

Effects of Herbaceous Plant Roots on the Soil Shear Strength of the Collapsing Walls of Benggang in Southeast China

Fang Shuai ^{1,†}, Mengyuan Huang ^{2,†}, Yuanyuan Zhan ¹, Qin Zhu ¹, Xiaolin Li ¹, Yue Zhang ¹, Jinshi Lin ¹, Yanhe Huang ¹ and Fangshi Jiang ^{1,*}

¹ Jinshan Soil and Water Conservation Research Center, Fujian Agriculture and Forestry University, Fuzhou 350002, China

² College of Energy, Xiamen University, Xiamen 361005, China

* Correspondence: jfsfafu@163.com; Tel.: +86-137-0936-1097

† These authors contributed equally to this work.

Abstract: Failure of collapsing walls is an important process affecting the development of Benggang and is closely related to the soil shear strength. Plant roots can increase the soil shear strength. However, the effects and mechanisms of root reinforcement on the soil shear strength of collapsing walls remain unclear. To explore the shear strength characteristics of collapsing walls and their influencing factors under different vegetation conditions, *Pennisetum sinense*, *Dicranopteris dichotoma*, *Odontosoria chinensis*, and *Neyraudia reynaudiana* were adopted as experimental objects in the Benggang district of Anxi County, Southeast China. We measured the root characteristics and in situ shear strength of root–soil complexes by dividing soil with the four vegetation conditions into five soil layers: 0–5 cm, 5–10 cm, 10–15 cm, 15–20 cm, and 20–25 cm. The average shear strength of the root–soil complexes of the various plants ranked as follows: *Pennisetum sinense* (30.95 kPa) > *Odontosoria chinensis* (28.08 kPa) > *Dicranopteris dichotoma* (21.24 kPa) > *Neyraudia reynaudiana* (14.99 kPa) > bare soil (11.93 kPa). The enhancement effect of the root system on the soil shear strength was mainly manifested in the 0–5 cm soil surface layer. The soil shear strength attained an extremely significant positive correlation with the root length density, root surface area density, root volume density, root biomass density, for root diameters (L) less than or equal to 0.5 mm and between 0.5 and 1 mm, the soil shear strength could be simulated by using root volume density. The shear strength of undisturbed root–soil complexes measured with a 14.10 pocket vane tester was higher than the value obtained with the Wu–Waldron model (WWM). The correction coefficient k' varied between 0.20 and 20.25, mostly exceeding 1, and the average correction coefficient k' value was 4.94. The average correction coefficient determined in this test can be considered to modify the WWM model when conducting experiments under similar conditions.

Keywords: gravity erosion; root–soil complex; soil mechanics; soil and water conservation; vegetation restoration



Citation: Shuai, F.; Huang, M.; Zhan, Y.; Zhu, Q.; Li, X.; Zhang, Y.; Lin, J.; Huang, Y.; Jiang, F. Effects of Herbaceous Plant Roots on the Soil Shear Strength of the Collapsing Walls of Benggang in Southeast China. *Forests* **2022**, *13*, 1843. <https://doi.org/10.3390/f13111843>

Academic Editors: Yang Yang, Andrey Soromotin, Tongchuan Li and Jiangbo Qiao

Received: 29 September 2022

Accepted: 1 November 2022

Published: 4 November 2022

Publisher's Note: MDPI stays neutral with regard to jurisdictional claims in published maps and institutional affiliations.



Copyright: © 2022 by the authors. Licensee MDPI, Basel, Switzerland. This article is an open access article distributed under the terms and conditions of the Creative Commons Attribution (CC BY) license (<https://creativecommons.org/licenses/by/4.0/>).

1. Introduction

Benggang is a phenomenon involving the erosion and collapse of hillside soil or rock masses due to the action of water flow and gravity, mainly occurring in the red soil hilly region of southern China, where the desilicization and iron-rich aluminization of the soil are obvious due to sufficient water and a hot and humid climate, giving the soil a red coloration [1]. According to survey statistics of China's Ministry of Water Resources in 2005, there are 239,100 Benggang units in the red soil region of South China, covering an area of 1220 km², largely distributed in Guangdong, Fujian, Jiangxi, Hubei, Hunan, Anhui, and Guangxi provinces (autonomous regions) in Southeast China [1]. Benggang occurs very suddenly and quickly; the amount of erosion is large, and the erosion modulus of soil is 50 kt km² yr⁻¹, which is 50 times that of gently sloping areas [1,2]. Severe soil

erosion destroys mountains and produces large amounts of sediment that can destroy farmland, silt rivers and reservoirs, and wash away roads, causing notable damage to the local environment [3,4]. The direct economic loss due to Benggang in the red soil region of South China amounted to CNY 20.5 billion (USD 2.86 billion), and the affected population reached 9.17 million people from 1949 to 2005 [1]. Benggang mainly comprises four parts: the upper catchment, collapsing wall, colluvial deposit, and alluvial fan (Figure 1) [5]. Among these parts, the failure process of collapsing walls is the most critical process in Benggang development, which is closely related to the decline in soil shear strength [3,6]. Therefore, the study of the collapsing wall shear strength and its influencing factors is of great relevance for revealing the collapse process of collapsing walls and establish effective treatment measures for Benggang.



Figure 1. Photo of Benggang in the study area. (a,b) The Benggang scene before the treatment in 2012; (c,d) The Benggang scene after the treatment in 2020.

Vegetation restoration is an effective means to prevent and control Benggang, and plant roots, in particular, play an important role in this process. Plant roots are materials with high polymer structures and are composed of root epidermis and internal fibers, giving them a high tensile strength. Soil has compressive resistance, and when roots grow in a crisscross manner in soil and are combined with soil to form root–soil complexes, the soil is strengthened via thick root anchoring and fine root reinforcement [7]. The root tensile strength is combined with the compressive strength of soil to jointly resist

external shear stress, improve soil mechanical properties, and enhance the shear resistance of soil when root–soil complexes are subjected to external loads [8,9]. Trees, shrubs, and herbaceous plants improve the soil shear strength at different soil depths [10–16]. Among them, the herbaceous root system is mostly distributed near the surface, and the root system is well developed, thin, and luxuriant, developing a wide contact area with soil, and exerting a highly significant effect on restraining soil displacement on shallow slopes and improving slope stability [17–21]. Comino and Druetta [22] studied herbaceous plants such as *Festuca pratensis* and *Lolium perenne* and demonstrated that the shear strength of the root–soil complexes of these herbaceous plants was 50–325% higher than that of soil without roots. Meanwhile, studies have shown that in terms of the inhibition of soil displacement of 0–40 cm shallow slope layers, the improvement in soil reinforcement attributed to the root system of herbs was approximately 3–10 times that attributed to the system of shrubs [12,23]. The enhancement effect of the root system on the shear strength of root–soil complexes is mainly reflected in the influence of root architecture parameters and tensile properties. In terms of the study on the relationship between root architecture parameters and the shear strength of root–soil complexes, Mokhammad [24] reported that the root volume density was closely related to soil shear strength improvement through the direct shear tests of bamboo root–soil complexes. Ajedegba et al. [8] and Huang et al. [9] showed that the root weight density significantly contributed to the shear strength of root–soil complexes, and there was an optimal root content in regard to the influence of roots on cohesion. Mahannopkul and Jotisankasa [25] proposed that the observed increase in the shear strength of root–soil complexes was primarily determined by the root length density and root biomass. Loades et al. [18] demonstrated that *Hordeum vulgare* roots could improve the shear strength of root–soil complexes and proposed that this improvement was closely related to the tensile characteristics of roots. Mattia et al. [12] suggested that the higher the root tensile strength of plants is, the greater the enhancement in the root–soil complex cohesion. However, due to the influence of plant genetic properties and the growth environment, different plant roots can exert different effects on the soil shear strength. Thus, the soil consolidation effect and mechanism of different plant species must be studied further.

To conveniently calculate the strengthening effect of roots on the soil shear strength, many scholars have proposed models to calculate the shear strength of root–soil complexes, such as the Wu–Waldron model (WWM) [26,27], Fiber Bundle Model (FBM) [28], and Root Bundle Model weibull (RBMw) [29]. The WWM model indicates that when root–soil complexes are subjected to external forces, roots in soil can simultaneously break [22,30]. On this basis, the FBM model introduces the fiber bundle theory of composite fracture mechanics into the field of root–soil fixation. According to the model, all the roots passing through the shear plane fracture continuously according to the bearing capacity under external load [15]. RBMw is an extended version of FBM and a survival function that covers the sundry mechanical properties of roots [15,28]. Among these models, the WWM model has been widely used due to its small number of parameters and simple calculation process. However, since the increment of the predicted value of the shear strength of WWM model is usually higher than the actual measured value [9,30], the model must be modified. Moreover, there are notable differences in the properties of different root–soil complexes, resulting in large differences in model correction coefficients [9,28], so it is necessary to conduct further related research. Moreover, studies on existing WWM models largely focus on direct shear tests of remolded soil of Benggang [7,9], which destroys the original structure of the root–soil complexes under field conditions and cannot truly and comprehensively reflect the characteristics of undisturbed soil. Therefore, in situ shear tests under field conditions should be performed to modify and improve the WWM model for undisturbed root–soil complexes and provide a basis for the extension and application of this model.

At present, there have been studies on the shear strength of remolded root–soil complexes on collapsing walls in Benggang [7,9], whereas the research of the shear strength

of undisturbed root–soil complexes in the field is limited. To this end, in this study, four species of herbs, i.e., *Pennisetum sinense*, *Dicranopteris dichotoma*, *Odontosoria chinensis*, and *Neyraudia reynaudiana* (Figure 2), common in the Benggang area of southern China, were used as research objects, and in situ shear tests were conducted. The main research purposes were as follows: (1) to determine the root architecture and tensile characteristics of these four herbaceous plants; (2) to determine the difference in the shear strength of the root–soil composites of these four species of herbaceous plants and its influencing factors; and (3) to modify the WWM model to obtain the shear strength of the root–soil complexes of these four species of herbaceous plants. The research results could enrich the understanding of the mechanism of different vegetation types in controlling the collapse of collapsing walls, provide a basis to fully understand the soil and water conservation functions of collapsing wall vegetation, and establish a reference for the selection, optimization, and configuration of collapsing wall prevention measures.

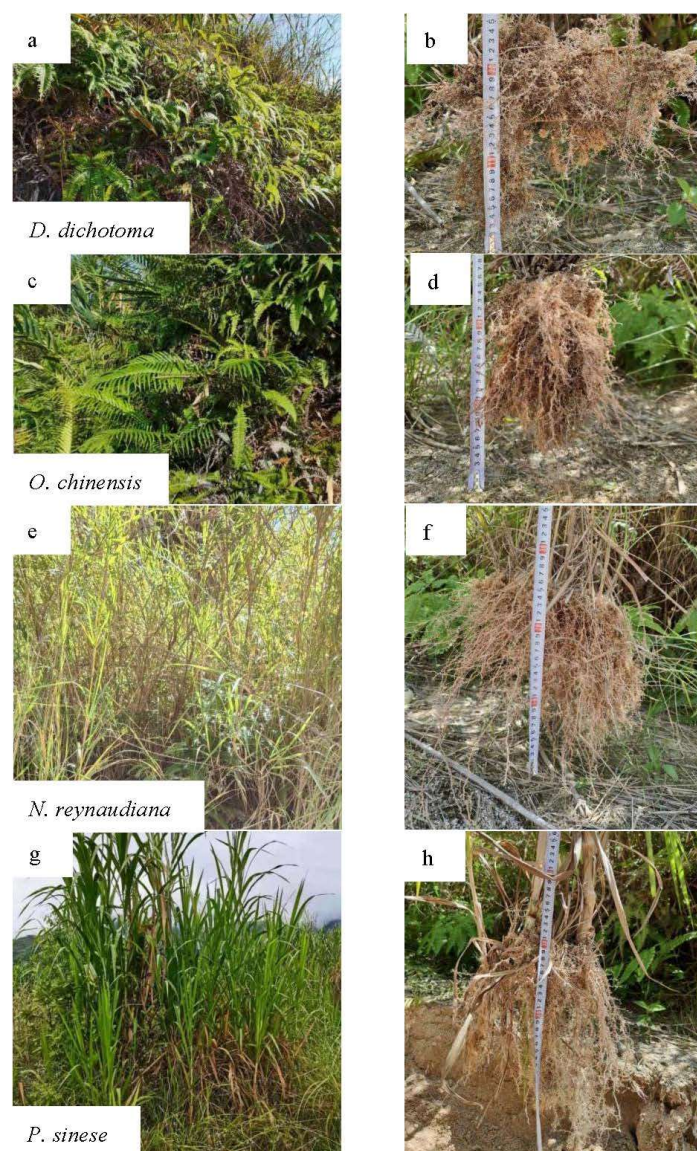


Figure 2. (a) Growth of *Dicranopteris dichotoma*; (b) Root system of *Dicranopteris dichotoma*; (c) Growth of *Odontosoria chinensis*; (d) Root system of *Odontosoria chinensis*; (e) Growth of *Neyraudia reynaudiana*; (f) Root system of *Neyraudia reynaudiana*; (g) Growth of *Pennisetum sinense*; (h) Root system of *Pennisetum sinense*.

2. Materials and Methods

2.1. Study Area

Test samples were collected in Yangkeng village, Longmen town, Anxi County, Fujian Province, with a geographical location of 24°57' N and 118°05' E and an average altitude of 201 m (Figure 3). The region exhibits a subtropical monsoon climate with high temperatures and a rainy season in summer (May–September), with an average annual rainfall of 1800 mm and an annual average temperature of 19 °C. The rocks in this area mainly comprise coarse-grained granite, forming deep weathering crusts under the action of high temperatures and rainfall. Weathering crusts exhibit a high coarse grain content, poor structure, and low corrosion resistance. Under the action of precipitation and gravity, slopes are prone to scouring and collapse, resulting in the formation of Benggang landforms. According to 2005 survey data, the Yangkeng village experiences serious Benggang erosion. The number of Benggang landforms is 226, and the density is 40 km⁻², which is 10 times that in Anxi County and 200 times that in Fujian Province. According to the study, the annual soil loss in the area is more than 60 KT [1]. Therefore, the Benggang erosion phenomenon in Yangkeng village is representative of southern China [1]. There is a single vegetation type typical of the study area. The main tree species include *Pinus massoniana* and *Eucalyptus robusta*. Understory shrub species largely include *Melastoma candidum*, *Rhodomyrtus tomentosa*, and *Syzygium buxifolium*. The dominant herbaceous plants include *Dicranopteris dichotoma*, *Neyraudia reynaudiana*, *Odontosoria chinensis*, and *Pennisetum sinense*. These plant species exhibit well-developed roots and provide suitable soil and water conservation functions, which can effectively hold soil and prevent failure of collapsing walls.

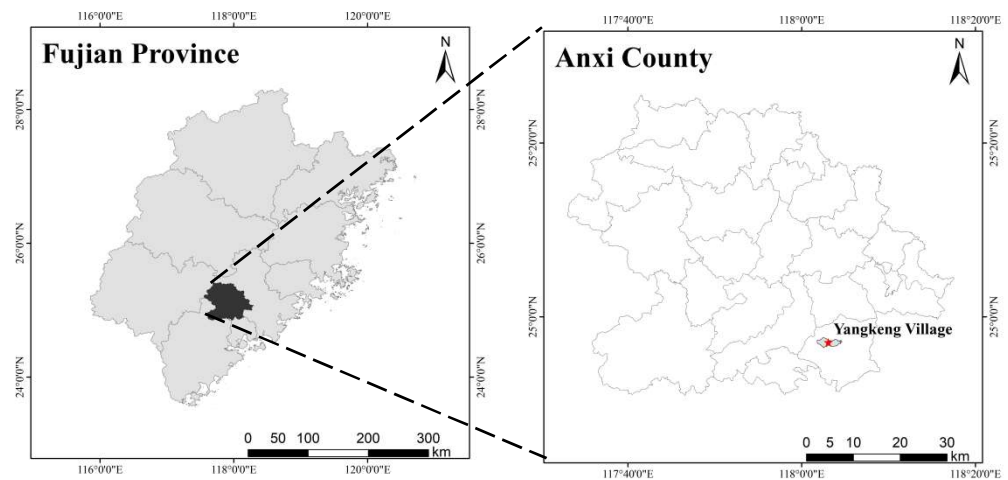


Figure 3. Location of the research site.

2.2. Field Investigation and Shear Strength Determination of Root–Soil Complexes

A Benggang site treated in 2012 was selected in Yangkeng village, and an investigation was performed in August 2020. We have been conducting field research in Yangkeng village for a long time. During this process, we found that the dominant herbaceous species at Yangkeng village included *Pennisetum sinense*, *Dicranopteris dichotoma*, *Odontosoria chinensis* and *Neyraudia reynaudiana*, and these four species were therefore selected as the research objects. A uniform collapsing wall with satisfactory vegetation growth and a relatively consistent vegetation composition was selected in the Benggang area. Three sample plots were established for each vegetation and bare land, and the area of each sample plot was 2 m × 2 m. The vegetation coverage, average plant height, number of plants per unit area, and root depth were investigated in the established sample plots, as summarized in Table 1. Vegetation coverage was measured by digital camera photography. Field investigation demonstrated that herb roots in the test area could grow to reach a depth of approximately 25 cm below the surface [9], so the soil depth in this test ranged from 0 to 25 cm, which was

divided into five soil layers of 0–5 cm, 5–10 cm, 10–15 cm, 15–20 cm, and 20–25 cm for shear strength measurement purposes.

Table 1. Basic situation of vegetation types in the sample plot.

Vegetation Types	Average Plant Height/cm	Average Crown/cm	Average Depth of the Root/cm	Average Vegetation Coverage/%
<i>Dicranopteris dichotoma</i>	28 ± 9	17 ± 5	16 ± 3	95
<i>Odontosoria chinensis</i>	82 ± 21	72 ± 18	25 ± 2	98
<i>Neyraudia reynaudiana</i>	260 ± 14	51 ± 2	26 ± 2	90
<i>Pennisetum sinense</i>	233 ± 29	61 ± 7	24 ± 2	90

Note: Data in the table are the mean ± standard deviation.

In each of the three plots of four vegetation, a plant with good growth and relatively good consistency was selected for the determination object. The shear strength of root–soil complexes was measured with a 14.10 pocket vane tester (Figure 4), which is mainly composed of a torque meter and three different measuring range values of 0–0.2, 0–1, and 0–2.5 kg cm² of the blade each [31–34]. In this experiment, a blade with a range of 0–1 kg cm² was used. The smallest division on the dial is 0.05 kg cm², permitting visual interpretation to the nearest 0.01 kg m². The total measurement ranged from 0 to 250 kPa. This instrument can measure the same soil sample or stratum several times within a short period and calculate the average value. The procedure entails the insertion of a shaft with blades into the soil, after which the shaft is rotated at a certain speed and force. The force can be measured at the tensile fracture point of the tested soil, and the shear value at this point can be calculated. Surface crusts around vegetation stems were removed, and the shear strength of the above five soil layers in each plot was measured with the 14.10 pocket vane tester. In bare soil, the surface layer with crusts was scraped off first, and then the shear strength was measured. Considering that stratification and sampling at the same position could affect the properties of the underlying soil, measurements of the different soil layers were conducted along different plant extension directions. For example, the shear strength of the 0–5 cm soil layer was measured along the north direction of the plant, and the shear strength of the 5–10 cm soil layer was measured along the south direction. After the removal of plant stems and leaves, the 14.10 pocket vane tester was used to measure the shear strength vertically downwards along the plant roots. The shear strength of each layer was measured 10 times in total. After elimination of the maximum and minimum values, the average value was obtained as the shear strength value of each layer.

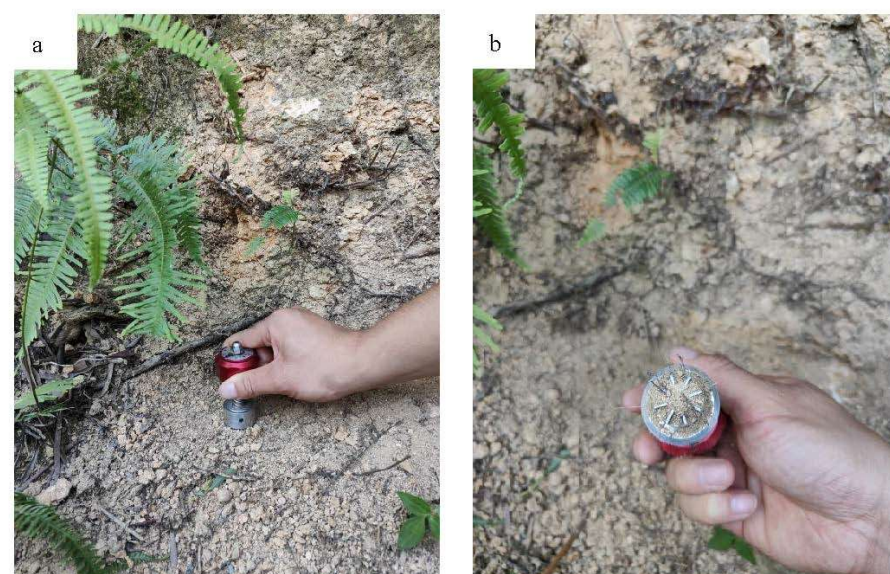


Figure 4. (a) Photo of the in situ direct shear test process; (b) photo after direct shearing.

2.3. Sample Collection and Determination

Soil samples used for the determination of the moisture content and bulk density and root samples were collected from the same soil layer and direction as those in the shear strength test. First, a ring cutter with a volume of 100 cm³ (with a base area of 20 cm² and a height of 5 cm) was used to collect undisturbed soil in layers within the sample plot. A total of 75 ring cutter samples were collected. Afterwards, the samples were returned to the laboratory, where they were immediately weighed and dried, and the data were used to calculate the soil moisture and bulk density. The total porosity was calculated by soil bulk density and density (2.65 g cm⁻³) [35]. The average values of soil bulk density and porosity in various layers were used as the basic values of the sample plots (Table 2). At the same time, in order to obtain the basic values of various sample plots, a total of 15 mixed samples were collected by the quincunx sampling method [35] at a depth of 25 cm. Chemical properties and particle composition of mixture samples were measured. Soil pH was measured by a pH meter (soil/water ratio = 1:2.5), organic matter was measured by potassium dichromate [35], and particle size distribution was measured according to Jackson [36]. The physical and chemical properties of basic soil are listed in Table 2.

Table 2. Soil properties in different vegetation lands.

Experiment Land	pH	Soil Organic Matter (g kg ⁻¹)	Soil Bulk Density (g cm ⁻³)	Total Porosity (%)	Particle Size Distribution/%			
					Gravel >2 mm	Sand 2–0.05 mm	Silt 0.05–0.002 mm	Clay <0.002 mm
Bare land	4.10 ± 0.32	3.05 ± 0.32	1.43 ± 0.20	45.87 ± 9.13	17.54 ± 1.78	49.92 ± 7.43	26.65 ± 4.74	5.89 ± 0.60
<i>D. dichotoma</i>	4.26 ± 0.25	4.28 ± 0.54	1.32 ± 0.20	50.37 ± 9.79	15.65 ± 1.98	49.40 ± 5.93	30.29 ± 3.11	4.66 ± 0.38
<i>O. chinensis</i>	4.64 ± 0.27	4.45 ± 0.31	1.29 ± 0.19	51.27 ± 9.67	14.15 ± 2.14	48.25 ± 7.17	32.68 ± 5.12	4.92 ± 0.89
<i>N. reynaudiana</i>	4.31 ± 0.21	3.85 ± 0.42	1.29 ± 0.18	51.43 ± 9.25	16.96 ± 2.33	42.30 ± 6.74	35.55 ± 4.52	5.19 ± 0.56
<i>P. sinense</i>	4.36 ± 0.18	5.02 ± 0.58	1.29 ± 0.19	51.31 ± 9.61	18.23 ± 2.20	46.56 ± 8.04	31.09 ± 5.39	4.12 ± 0.66

Root–soil complex samples were collected from the 0–5 cm, 5–10 cm, 10–15 cm, 15–20 cm, and 20–25 cm layers along the plant roots with a ring cutter (with a base area of 100 cm² and a height of 5 cm), with 3 repetitions for each layer. A total of 60 ring cutter samples were collected. The ring cutter was pressed vertically and slowly into the soil, the soil around the ring cutter was removed, and the root system outside the ring cutter was cut off with scissors to avoid damage to the ring cutter sample due to root pulling. Then, the collected ring cutter samples were covered with lids at both ends and fixed with rubber bands. After the ring cutter samples were transported to the laboratory, each root–soil complex sample was carefully removed and placed on a 0.05-mm mesh screen for slow washing until all roots were washed out [37]. The roots were slowly separated with tweezers, and the surface water of the roots was then dried. An Epson Perfection device was used for grey scanning at 300 dpi, and the root length, root surface area, root volume, and root biomass were obtained in the WinRHIZO (Pro. 2013e) root analysis system [37]. The scanned roots, contained in a paper envelope, were placed in an oven and dried at 65 °C until a constant weight was attained. Then, the roots were removed and weighed to obtain the root biomass data.

The determination of root components included lignin, cellulose, hemicellulose, and holocellulose. These root components were determined according to the Van Soest detergent fiber analysis method [38] and national and agricultural industry standards. The chemical composition and proportion of each microstructure are provided in Table 3. The microstructure characteristics of the roots of four herbaceous plants were obtained via the paraffin sectioning method [39]. The tissues in the obtained sections were observed, and the proportion of each microstructure was analyzed (Table 3).

Table 3. The chemical composition and microstructure characteristics of the four herbaceous species.

Vegetation Types	Chemical Composition					Microstructure Characteristics			
	Lignin (%)	Cellulose (%)	Hemicellulose (%)	Holocellulose (%)	Wood Fiber Ratio	Average Diameter (mm)	Epidermal Thickness (μm)	Cortical Thickness (μm)	Pericycle Thickness (μm)
<i>D. dichotoma</i>	25.1	39.9	8.9	48.8	0.63	0.49	31.26	146.67	4.87
<i>O. chinensis</i>	20.7	36.8	6.5	43.3	0.56	0.75	34.09	93.75	4.33
<i>N. reynaudiana</i>	20.7	39.9	14.8	54.7	0.52	0.51	6.23	62.83	7.58
<i>P. sinense</i>	16.3	37.7	9.0	46.6	0.43	0.62	8.64	80.26	8.68

2.4. Determination of the Tensile Properties of Roots

A YG (B) 026G-250 electronic fabric strength measurement instrument was used in the single-fiber tensile test, referring to the national standard method of GB/T14344-2008 (Chemical Fibre Filament Tensile Test Method). The maximum test force of the instrument reached 2500 N, the entire process was conducted in automatic shift mode, and the speed ranged from 0.001 to 1000 mm·min⁻¹. The instrument could be controlled via digital speed regulation, with an error of $\leq \pm 2\%$ and a test force and displacement accuracy of $\leq \pm 0.2\%$ [9]. According to previous experimental results of our laboratory, roots develop the best tensile property at a distance of 50 mm, which was thus adopted as the measurement distance in this test [9]. The collapse rate of collapsing walls in the field is relatively high, so the root tensile test adopted the fast shear approach, and the tensile rate was set to 10 mm min⁻¹. The maximum tensile force was obtained through repeated root tensile experiments. The root tensile strength can be calculated as follows:

$$T = 4F/\pi D^2, \quad (1)$$

where T is the root tensile strength (MPa), F is the maximum root tensile force (N), and D is the average root diameter (mm).

2.5. Calculation of the Correction Coefficient of the WWM Model

The shear strength models of root–soil complexes are mainly WWM, FBM, and RBMw so far. Among them, FBM and RBMw models need more parameters, which are difficult to obtain under the conditions of our laboratory. So, this study selects the WWM model, which is relatively simple to calculate and modify. Wu et al. [26] and Waldron [27] reported that the addition of roots mainly increased soil cohesion but imposed a negligible effect on the internal friction angle. Therefore, they proposed a widely used root–soil complex shear strength model, namely, the WWM model, which largely calculates the enhancement value of the soil shear strength attributed to roots as follows:

$$\Delta S = k \cdot t \cdot RAR, \quad (2)$$

where ΔS is the increment in the shear strength of the simulated root–soil composite (kPa), k is the model correction coefficient (usually 1.2), t is the root tensile strength (MPa), and RAR is the ratio of the root cross-sectional area calculated by Roberta et al. [40] (ratio of the root volume to the ring cutter volume).

The shear strength enhancement value measured in the field can be obtained as follows:

$$\Delta C_r = \tau_{rs} - c_s, \quad (3)$$

where ΔC_r is the actual measured increase in the root shear strength (kPa), τ_{rs} is the actual measured shear strength of the root–soil complex (kPa), and c_s is the in situ measured bare land soil cohesion (kPa).

The correction coefficient (k') of the WWM model can be determined as follows:

$$k' = \Delta C_r / \Delta S, \quad (4)$$

where k' is the correction coefficient of the WWM model, ΔC_r is the actual measured increase in the root shear strength (kPa), and ΔS is the increment in the shear strength of the simulated root–soil composite (kPa).

2.6. Validity Test of the Fitted Equation

The fitting effect of the equation can be tested by the coefficient of determination of equation (R^2) and the coefficient of validity of the model (NSE). The coefficient of determination of the equation (R^2) can be calculated using SPSS software. The coefficient of validity of the model (NSE) can be calculated as follows:

$$NSE = 1 - \frac{\sum(Q_i - Q_{ci})^2}{\sum(Q_i - Q_m)^2}, \quad (5)$$

where NSE is the coefficient of validity of the model, Q_i is the measured value of sample i , Q_{ci} is the simulated value of sample i , and Q_m is the average of the actual measurements. When $NSE \geq 0.70$, the simulation effect of the equation is better.

2.7. Data Analysis and Processing

Excel 2010 and SPSS 24.0 [41] were used to process the data. Excel 2010 was used to complete data arrangement and chart generation, while the “compare means” function in SPSS 24.0 was used to compare the means between the variables, and other functions were used to conduct Pearson correlation analysis, significant difference analysis, parameter testing, and regression analysis of each fitting equation.

3. Results

3.1. Soil and Root Properties

Figure 5a shows that the moisture content in each layer of soil with vegetation was higher than that in bare land, and the different plant species exerted varied effects on the soil water content. Among the four species, the average natural moisture content in the soil layer containing *Odontosoria chinensis* was the highest, at 21.54%, followed by *Dicranopteris dichotoma*, at 20.46%. The average soil natural moisture content for *Pennisetum sinense* was 20.42%, the average soil natural moisture content for *Neyraudia reynaudiana* was 18.95%, and that in bare land was the lowest, at 18.07%. Further analysis of Figure 5a revealed that under the different vegetation conditions, the soil moisture content gradually increased with increasing soil layer. As shown in Figure 5b, the soil bulk density of each layer with vegetation was lower than that of bare soil. The order of the average soil bulk density was as follows: bare soil (1.43 g cm^{-3}) > *Dicranopteris dichotoma* (1.32 g cm^{-3}) > *Odontosoria chinensis* (1.29 g cm^{-3}) \approx *Pennisetum sinense* (1.29 g cm^{-3}) \approx *Neyraudia reynaudiana* (1.29 g cm^{-3}).

The distribution of vegetation roots in the study area was statistically analyzed, and the results are shown in Table 4. Table 4 indicates that there were significant differences in the root distribution among the four plants in the five soil layers from 0 to 25 cm, and roots were mostly distributed in the 0–5 cm soil layer. Regression equation fitting was conducted between the soil depth and root morphological parameters of the four plants (Table 5). With the increasing soil depth, the root configuration parameters of the four plants showed different functional downwards trends. Table 4 also shows that different root parameters differ in the order of different plants. The order of the average root length density was as follows: *Odontosoria chinensis* > *Pennisetum sinense* > *Neyraudia reynaudiana* > *Dicranopteris dichotoma*. The order of the average root surface area density was *Odontosoria chinensis* > *Pennisetum sinense* > *Dicranopteris dichotoma* > *Neyraudia reynaudiana*. The order of the average root volume density was as follows: *Pennisetum sinense* > *Odontosoria chinensis* > *Dicranopteris dichotoma* > *Neyraudia reynaudiana*. The order of the average root biomass density was as follows: *Neyraudia reynaudiana* > *Odontosoria chinensis* > *Dicranopteris dichotoma* > *Pennisetum sinense*. The root length density of roots of different diameters decreased with the increasing soil depth (Figure 6), and significant differences ($p < 0.05$) were observed only for *Neyraudia reynaudiana* roots of different diameters in all five soil layers. Figure 6 also shows that the

roots of all plants mainly included fine roots [42] with root diameters (L) of $L \leq 0.5$ mm and $0.5 < L \leq 1$ mm (the WinRHIZO (Pro. 2013e) root analysis system can calculate the root diameter directly). The specific gravity of the root length density in these two diameter classes exhibited the following order: *Pennisetum sinese* (95.46%) > *Odontosoria chinensis* (94.82%) > *Neyraudia reynaudiana* (91.77%) > *Dicranopteris dichotoma* (73.79%).

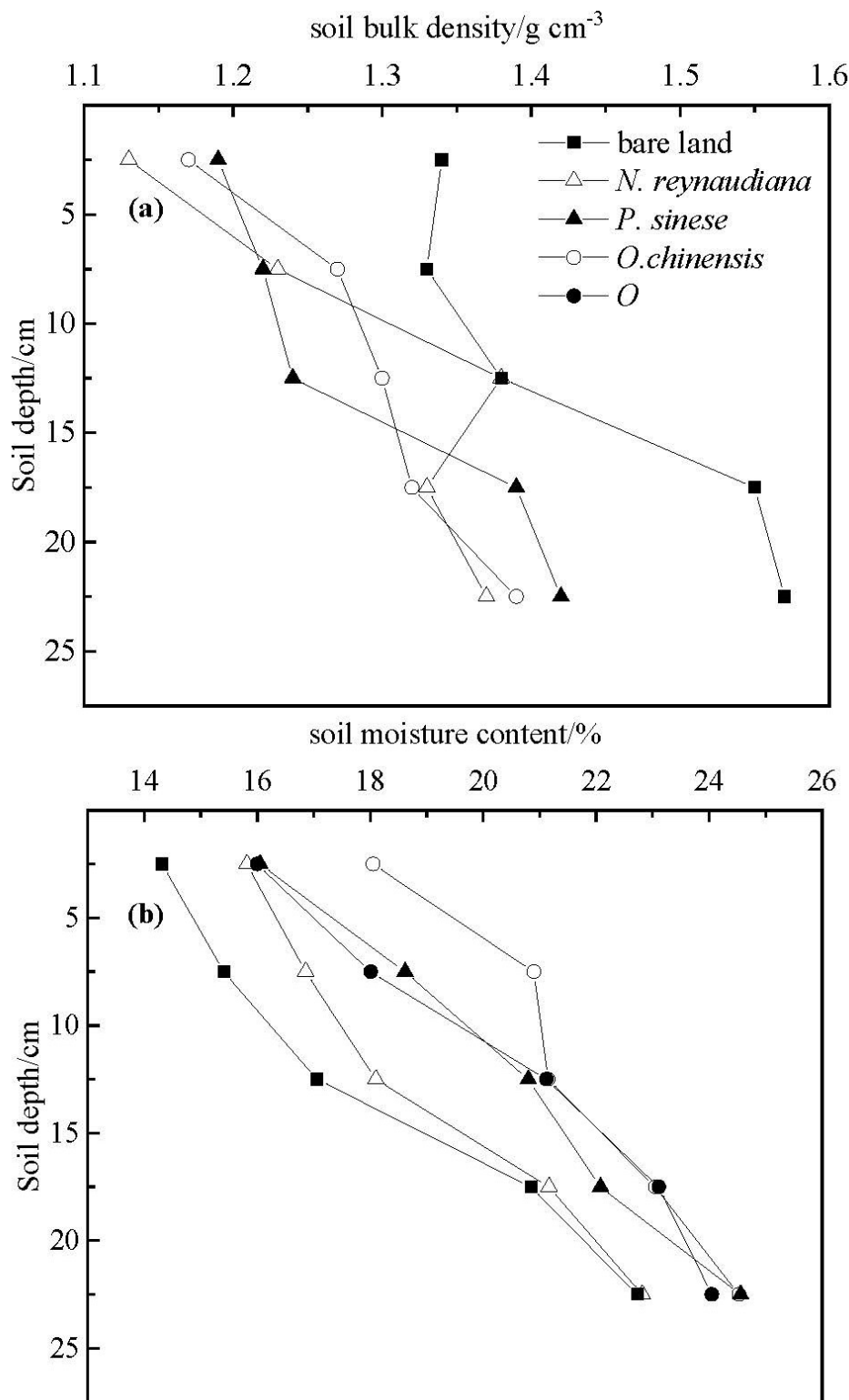


Figure 5. (a) Variation of soil moisture content with plant species. (b) Variation of soil bulk density with plant species.

Table 4. Root morphological parameters of the four herbaceous plants.

Vegetation Types	Soil Depth (cm)	Root Length Density (cm cm ⁻³)	Root Surface Density (cm ² 100 cm ⁻³)	Root Volume Density (cm ³ 100 cm ⁻³)	Root Biomass Density (g 100 cm ⁻³)
<i>N. reynaudiana</i>	0–5 cm	3.25 ± 0.41 a	7.17 ± 1.49 a	0.39 ± 0.19 a	1.28 ± 0.19 a
	5–10 cm	2.18 ± 0.21 b	4.80 ± 1.68 b	0.22 ± 0.15 b	0.92 ± 0.29 b
	10–15 cm	1.86 ± 0.46 c	4.10 ± 3.29 c	0.14 ± 0.11 c	0.64 ± 0.13 c
	15–20 cm	1.68 ± 0.68 d	3.71 ± 2.77 d	0.12 ± 0.06 d	0.48 ± 0.22 d
	20–25 cm	1.07 ± 0.46 e	2.36 ± 1.41 e	0.05 ± 0.06 e	0.19 ± 0.06 e
	Average	2.01	4.43	0.18	0.70
<i>P. sinense</i>	0–5 cm	3.98 ± 0.23 a	11.85 ± 0.32 a	1.32 ± 0.03 a	0.88 ± 0.62 a
	5–10 cm	2.71 ± 0.68 b	6.08 ± 0.59 b	0.85 ± 0.25 b	0.55 ± 0.29 b
	10–15 cm	1.94 ± 0.59 c	3.52 ± 1.56 c	0.48 ± 0.15 c	0.37 ± 0.15 c
	15–20 cm	1.36 ± 0.19 d	2.80 ± 0.04 d	0.39 ± 0.04 d	0.35 ± 0.22 d
	20–25 cm	1.03 ± 0.29 e	1.07 ± 0.46 e	0.05 ± 0.05 e	0.24 ± 0.21 e
	Average	2.20	5.06	0.62	0.48
<i>O. chinensis</i>	0–5 cm	7.93 ± 4.33 a	20.48 ± 9.45 a	1.06 ± 0.15 a	1.28 ± 0.26 a
	5–10 cm	4.12 ± 0.20 b	13.26 ± 2.71 b	0.57 ± 0.09 b	0.98 ± 0.23 b
	10–15 cm	3.03 ± 1.01 c	10.93 ± 1.56 c	0.44 ± 0.08 c	0.64 ± 0.24 c
	15–20 cm	1.50 ± 0.28 d	5.21 ± 2.54 d	0.26 ± 0.08 d	0.29 ± 0.22 d
	20–25 cm	0.83 ± 0.16 e	3.81 ± 2.33 e	0.08 ± 0.02 e	0.21 ± 0.08 e
	Average	3.48	10.74	0.48	0.68
<i>D. dichotoma</i>	0–5 cm	4.06 ± 1.17 a	11.37 ± 3.58 a	0.81 ± 0.38 a	1.37 ± 1.05 a
	5–10 cm	2.87 ± 0.87 b	6.56 ± 3.11 b	0.52 ± 0.35 b	0.87 ± 0.53 b
	10–15 cm	1.78 ± 0.53 c	3.12 ± 1.37 c	0.33 ± 0.21 c	0.45 ± 0.27 c
	15–20 cm	0.62 ± 0.47 d	1.69 ± 1.03 d	0.19 ± 0.13 d	0.31 ± 0.14 d
	20–25 cm	0.12 ± 0.05 e	0.68 ± 0.11 e	0.11 ± 0.04 d	0.12 ± 0.05 e
	Average	1.89	4.68	0.39	0.62

Note: Data in the table are mean ± standard deviation; Different lowercase letters indicate significant differences among different herb types in the same soil layer ($p < 0.05$).

Table 5. The equation of root morphological parameters of four kinds of vegetation types varying with the soil layer (h).

Vegetation Types	Root Length Density	Root Surface Area Density	Root Volume Density	Root Biomass Density
<i>N. reynaudiana</i>	$Rld = -0.91\log(h) + 4.09$ $R^2 = 0.97^{**}$	$Rsad = -2\log(h) + 9.01$ $R^2 = 0.97^{**}$	$Rvd = -0.15\log(h) + 0.52$ $R^2 = 0.99^{**}$	$Rbd = -0.05h + 1.36$ $R^2 = 0.99^{**}$
<i>P. sinense</i>	$Rld = 4.59e^{-0.07h}$ $R^2 = 0.99^{**}$	$Rsad = -4.81\log(h) + 16.07$ $R^2 = 0.99^{**}$	$Rvd = -0.55\log(h) + 1.87$ $R^2 = 0.97^{**}$	$Rbd = -0.29\log(h) + 1.13$ $R^2 = 0.99^{**}$
<i>O. chinensis</i>	$Rld = -3.21\log(h) + 10.82$ $R^2 = 0.99^{**}$	$Rsad = -7.57\log(h) + 28.05$ $R^2 = 0.96^{**}$	$Rvd = -0.43\log(h) + 1.45$ $R^2 = 0.99^{**}$	$Rbd = -0.06h + 1.39$ $R^2 = 0.97^{**}$
<i>D. dichotoma</i>	$Rld = -0.20h + 4.42$ $R^2 = 0.98^{**}$	$Rsad = -4.99\log(h) + 16.09$ $R^2 = 0.99^{**}$	$Rvd = 1.09e^{-0.10h}$ $R^2 = 0.99^{**}$	$Rbd = -0.57\log(h) + 1.93$ $R^2 = 0.99^{**}$

Note: Rld is the root length density. $Rsad$ is the root surface area density. Rvd is the root volume density. Rbd is the root biomass density, h is the soil layer. ** in the table represents an extremely significant correlation between fitting equations of the root morphological parameters of different herbaceous vegetation ($p < 0.01$), $n = 5$.

The average tensile strength of the four plants exhibited the order of *Neyraudia reynaudiana* > *Pennisetum sinense* > *Odontosoria chinensis* > *Dicranopteris dichotoma* (Table 6). There were significant differences in the average tensile strength among *Neyraudia reynaudiana*, *Pennisetum sinense*, and *Odontosoria chinensis*, but there were no significant differences in the average tensile strength between *Odontosoria chinensis* and *Dicranopteris dichotoma*.

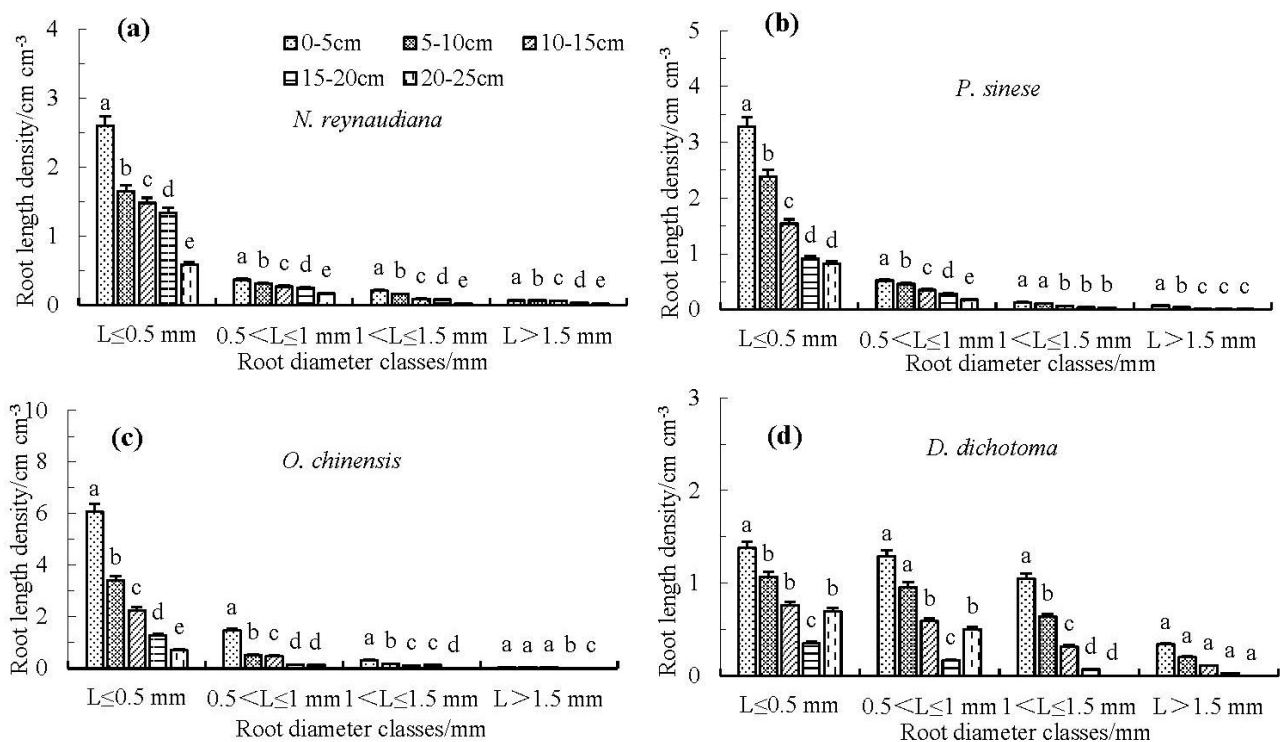


Figure 6. Comparison of root length density with different root diameter classes of *Neyraudia reynaudiana* (a), *Pennisetum sinense* (b), *Odontosoria chinensis* (c), and *Dicranopteris dichotoma* (d). Significant differences between experiments are denoted by different letters.

Table 6. Average tensile strength of different vegetation types.

Vegetation Types	Average Diameter (mm)	Average Tensile Strength (MPa)
<i>D. dichotoma</i>	0.49	18.42 ± 9.63 c
<i>N. reynaudiana</i>	0.75	61.35 ± 31.35 a
<i>O. chinensis</i>	0.51	19.65 ± 10.30 c
<i>P. sinense</i>	0.62	56.52 ± 19.11 b

Note: The average tensile strength in the table is mean ± standard deviation; Different lowercase letters indicated that the difference of root tensile strength of different grass species reached significant level ($p < 0.05$).

3.2. The Shear Strength of Root–Soil Complexes

Figure 7 shows that the shear strength of the vegetated areas was higher than that of bare land. The order of the average shear strength under each vegetation condition was as follows: *Pennisetum sinense* (30.95 kPa) > *Odontosoria chinensis* (28.08 kPa) > *Dicranopteris dichotoma* (21.24 kPa) > *Neyraudia reynaudiana* (14.99 kPa) > bare land (11.93 kPa). Moreover, there were significant differences among *Pennisetum sinense*, *Odontosoria chinensis*, *Dicranopteris dichotoma*, *Neyraudia reynaudiana*, and bare land ($p < 0.05$). The root system strengthened the soil and enhanced the soil shear strength. The promotion effect of *Pennisetum sinense* was the most obvious, which was approximately 2.6 times that of bare land, followed by *Odontosoria chinensis*, with an enhancement effect 2.4 times that of bare land, while the enhancement effect of *Dicranopteris dichotoma* was approximately 1.8 times that of bare land and 1.3 times that of *Neyraudia reynaudiana*. The difference in the soil shear strength among the different vegetation conditions in the different soil layers is shown in Figure 8a. The figure shows that the average shear strength of the root–soil complexes of the four plants was higher than that of bare land. Among the different plants, except for the shear strength of the 5–10 cm layer, which was the highest for the *Odontosoria chinensis* root–soil complexes, the shear strength of the *Pennisetum sinense* root–soil complexes were the highest in the other soil layers.

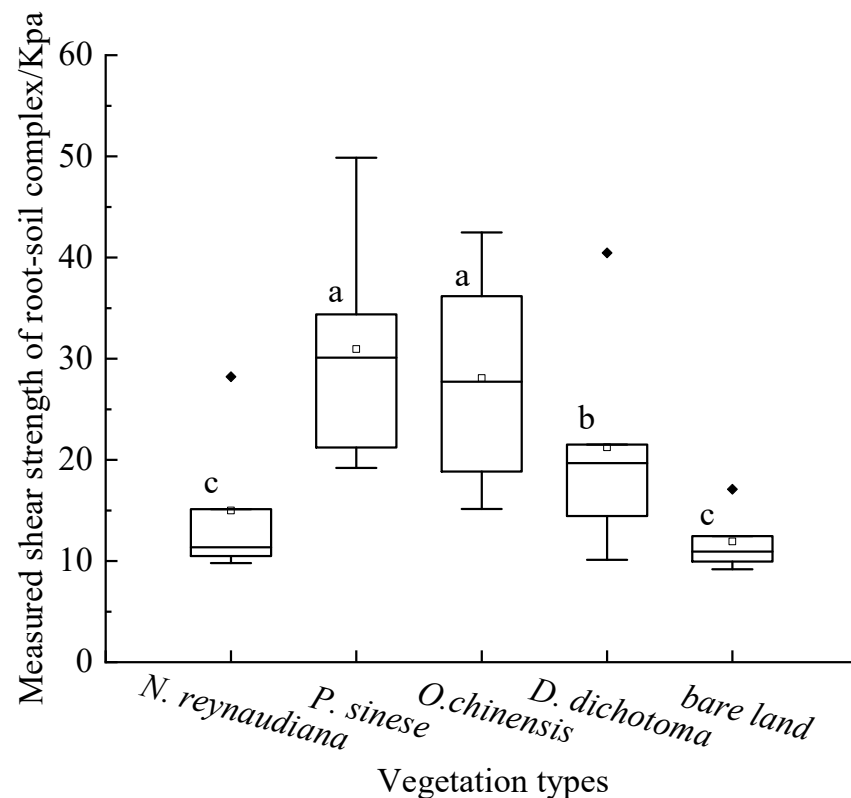


Figure 7. Comparison of soil shear strength under different vegetation types. Each box indicates the 25th/75th percentiles. The whisker caps represent the 10th/90th percentiles. The median is depicted by the line and the mean value is depicted by the square. For each vegetation, significant differences between experiments are denoted by different letters, such as a and a means no significant difference ($p > 0.05$), a–c means significant differences ($p < 0.05$).

The shear strength of the root–soil complexes of the different plants varied with the soil depth, as shown in Figure 8b. The diagram reveals that the strengthening effect of the root system was mainly concentrated in the 0–5 cm soil layer, and the shear strength of the root–soil complexes sharply decreased with the increasing soil depth. According to regression equation fitting between the shear strength of root–soil complexes and the soil depth (Table 7), it was found that the shear strength of bare soil and *Neyraudia reynaudiana* and *Dicranopteris dichotoma* root–soil complexes decreased with the increasing soil depth according to a power function, while that of the *Pennisetum sinese* root–soil complex decreased according to a logarithmic function and that of the *Odontosoria chinensis* root–soil complex decreased according to a linear function.

Table 7. Equation of the shear strength of the root–soil complex (SS) with soil layer (h).

Vegetation Types	Bare Land	<i>N. reynaudiana</i>	<i>P. sinese</i>	<i>O. chinensis</i>	<i>D. dichotoma</i>
Equation	$SS = 22.07h^{-0.28}$ $R^2 = 0.99^{**}$	$SS = 42.61h^{-0.49}$ $R^2 = 0.98^{**}$	$SS = -14.01\log(h) + 62.99$ $R^2 = 0.99^{**}$	$SS = -1.44h + 46.08$ $R^2 = 0.99^{**}$	$SS = 70.97h^{-0.58}$ $R^2 = 0.97^{**}$

Note: SS is the shear strength of the root–soil complex, h is the soil layer. ** in the table indicates that the fitting equations of shear strength of different herbaceous vegetation are highly significantly correlated ($p < 0.01$), $n = 5$.

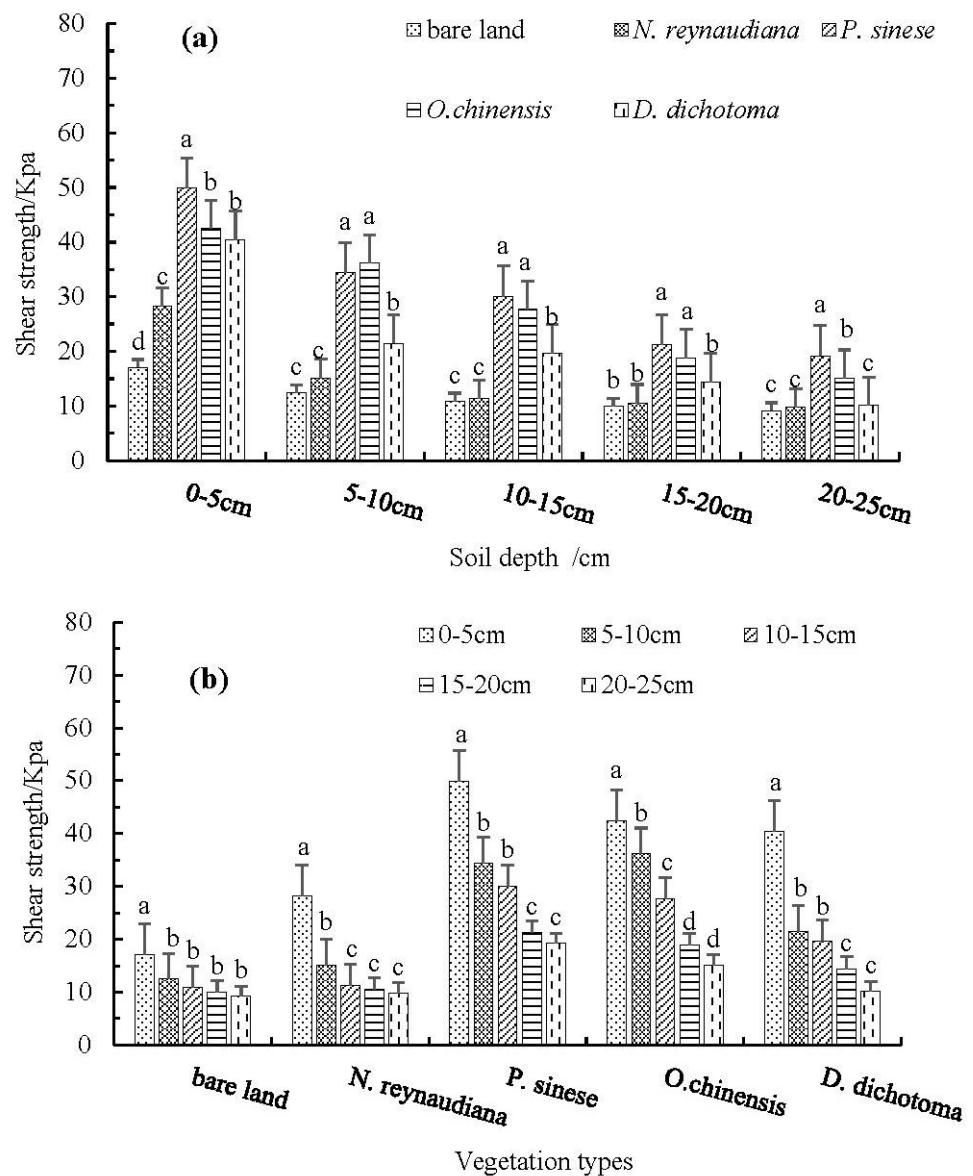


Figure 8. (a) Differences in shear strength of the vegetation types under different soil layers; (b) Soil shear strength of different vegetation types varying with soil depth. Significant differences between experiments are denoted by different letters.

3.3. Relationship between Shear Strength and Soil and Root Properties

To obtain the main factors of the root–soil complexes, correlation analysis was conducted on the root parameters, soil properties, and shear strength, and the results are listed in Table 8. The table reveals that the shear strength was significantly positively correlated with the root length density, root surface area density, root volume density, and root biomass density. There was a significant negative correlation between the shear strength of the plant root–soil complexes and the soil bulk density.

Table 8. Correlation coefficient between the root parameters, soil properties, and shear strength.

Indicators	Shear Strength	Root Length Density	Root Surface Density	Root Volume Density	Root Biomass Density	$L \leq 0.5$ mm	$0.5 < L \leq 1$ mm	$1 < L \leq 1.5$ mm	$L > 1.5$ mm	Tensile Strength	Bulk Density	Moisture Content
Shear strength	1											
Root length density	0.80 **	1										
Root surface density	0.80 **	0.96 **	1									
Root volume density	0.94 **	0.79 **	0.78 **	1								
Root biomass density	0.67 **	0.83 **	0.78 **	0.64 **	1							
$L \leq 0.5$ mm	0.74 **	0.93 **	0.91 **	0.73 **	0.68 **	1						
$0.5 < L \leq 1$ mm	0.61 **	0.80 **	0.74 **	0.66 **	0.71 **	0.58 **	1					
$1 < L \leq 1.5$ mm	0.42	0.47 *	0.43	0.42	0.67 **	0.12	0.78 **	1				
$L > 1.5$ mm	0.37	0.37	0.33	0.38	0.65 **	0.2	0.68 **	0.97 **	1			
Tensile strength	−0.10	−0.15	−0.29	−0.07	−0.05	−0.04	−0.43	−0.38	−0.27	1		
Bulk density	−0.75 **	−0.76 **	−0.70 **	−0.73 **	−0.86 **	−0.65 **	−0.62 **	−0.57 **	−0.53 *	−0.08	1	
Moisture content	−0.59 **	−0.65 **	−0.56 *	−0.65 **	−0.87 **	−0.52 *	−0.54 *	−0.56 **	−0.61 **	−0.26	0.85 **	1

Note: * in the table represents a significant correlation ($p < 0.05$), ** represents an extremely significant correlation ($p < 0.01$), $n = 20$.

Equation fitting of the shear strength of the root–soil complexes with the root indexes that were positively correlated and the soil properties is shown in Figure 9 and Table 9. As seen from the figure and table, the shear strength of the root–soil complexes varied with root length density, root surface area density, root volume density, root biomass density, $L \leq 0.5$ mm, $0.5 < L \leq 1$ mm, soil bulk density, and moisture content, mostly as exponential or power functions, with a few as linear or logarithmic functions. $p < 0.01$ for all equations indicates that the fitting effect of the equations was beneficial. Linear stepwise regression fitting was performed between the shear strength and different root and soil indexes. All equations reached the extremely significant level, and the results are listed in Table 10. Table 10 shows that the dominant factors of the shear strength of *Neyraudia reynaudiana* root–soil complexes included the root volume density (*Rvd*) and roots with a root diameter of $0.5 < L \leq 1$ mm ($L_{0.5-1}$). The factor dominating the shear strength of *Pennisetum sinense* root–soil complexes was the root length density (*Rld*). The dominant factor of the shear strength of *Odontosoria chinensis* root–soil complexes was the root biomass density (*Rbd*). The root volume density (*Rvd*) and soil moisture content (*Swc*) were the main influencing factors of the shear strength of *Dicranopteris dichotoma* root–soil complexes. Considering all root–soil complexes, the root volume density (*Rvd*) exerted the greatest influence on the shear strength of root–soil complexes.

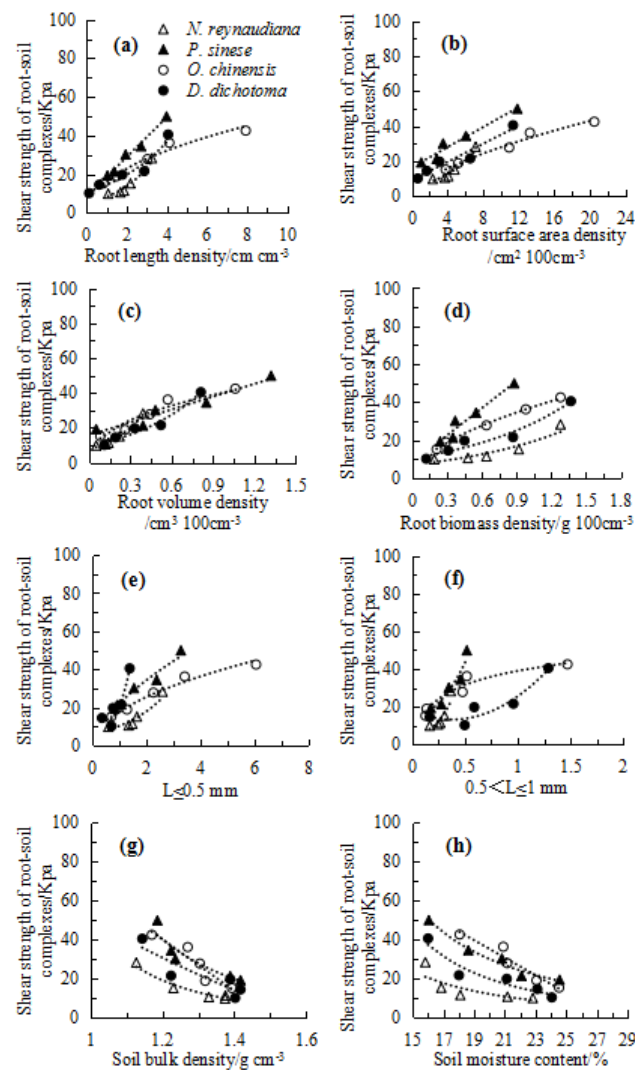


Figure 9. Relationship between the shear strength of the root–soil complexes and root length density (a), root surface area density (b), root volume density (c), root biomass density (d), root diameter (L) of less than or equal to 0.5 mm (e), root diameter (L) between 0.5 and 1 mm (f), soil bulk density (g), and soil moisture content (h).

Table 9. Fitting equations of the shear strength of the root–soil complex (SS) and root indicators.

Indicators	Vegetation Types	Dominant Factor Equation	R ²	Indicators	Vegetation Types	Dominant Factor Equation	R ²
Root length density /cm cm ⁻³	<i>N. reynaudiana</i>	$SS = 4.84e^{0.52Rld}$	0.93 **	$L \leq 0.5 \text{ mm}$	<i>N. reynaudiana</i>	$SS = 5.87e^{0.56L_{0.5}}$	0.86 *
	<i>P. sinese</i>	$SS = 10.33Rld + 8.18$	0.99 **		<i>P. sinese</i>	$SS = 22.08L_{0.5}^{0.63}$	0.97 **
	<i>O. chinensis</i>	$SS = 16.34Rld^{0.49}$	0.98 **		<i>O. chinensis</i>	$SS = 17.84L_{0.5}^{0.51}$	0.98 **
	<i>D. dichotoma</i>	$SS = 10.62e^{0.31Rld}$	0.94 **		<i>D. dichotoma</i>	$SS = 25.35L_{0.5} - 0.35$	0.72
Root surface area density/cm ² 100 cm ⁻³	<i>N. reynaudiana</i>	$SS = 4.84e^{0.24Rsd}$	0.93 **	$0.5 < L \leq 1 \text{ mm}$	<i>N. reynaudiana</i>	$SS = 3.27e^{5.25L_{0.5}-1}$	0.80 *
	<i>P. sinese</i>	$SS = 2.87Rsd + 16.45$	0.96 **		<i>P. sinese</i>	$SS = 11.01e^{2.72L_{0.5}-1}$	0.93 **
	<i>O. chinensis</i>	$SS = 6.65Rsd^{0.62}$	0.98 **		<i>O. chinensis</i>	$SS = 10.91\ln(L_{0.5-1}) + 39.01$	0.94 **
	<i>D. dichotoma</i>	$SS = 2.60Rsd + 9.09$	0.94 **		<i>D. dichotoma</i>	$SS = 23.26L_{0.5-1} + 4.92$	0.75
Root volume density/cm ³ 100 cm ⁻³	<i>N. reynaudiana</i>	$SS = 7.53e^{3.29Rvd}$	0.98 **	Soil bulk density /g cm ⁻³	<i>N. reynaudiana</i>	$SS = 46.60Sbd^{-4.88}$	0.93 **
	<i>P. sinese</i>	$SS = 24.55Rvd + 15.78$	0.94 **		<i>P. sinese</i>	$SS = 91.48Sbd^{-4.54}$	0.91 *
	<i>O. chinensis</i>	$SS = 40.69Rvd^{0.43}$	0.92 *		<i>O. chinensis</i>	$SS = -131.94Sbd + 198.46$	0.88 *
	<i>D. dichotoma</i>	$SS = 9.46e^{1.79Rvd}$	0.95 **		<i>D. dichotoma</i>	$SS = -107.4\ln(Sbd) + 50.29$	0.80 *
Root biomass density/g·100 cm ⁻³	<i>N. reynaudiana</i>	$SS = 6.93e^{0.98Rbd}$	0.89 *	Soil moisture content/%	<i>N. reynaudiana</i>	$SS = 14,644Smc^{-2.38}$	0.71
	<i>P. sinese</i>	$SS = 47.66Rbd + 8.17$	0.95 **		<i>P. sinese</i>	$SS = 29,978Smc^{-2.31}$	0.96 **
	<i>O. chinensis</i>	$SS = 36.57Rbd^{0.56}$	0.99 **		<i>O. chinensis</i>	$SS = -4.51Smc + 125.15$	0.93 **
	<i>D. dichotoma</i>	$SS = 10.25e^{0.99Rbd}$	0.93 **		<i>D. dichotoma</i>	$SS = 98,565Smc^{-2.844}$	0.90 *

Note: SS is the shear strength of the root–soil complex, *Rld* is the root length density, *Rsd* is the root surface area density, *Rvd* is the root volume density, *Rbd* is the root biomass density. $L_{0.5}$ is the root diameters less than or equal to 0.5 mm. $L_{0.5-1}$ is the root diameters between 0.5 and 1 mm. *Sbd* is the soil bulk density. *Smc* is the soil moisture content. * in the table represents a significant correlation ($p < 0.05$), ** represents an extremely significant correlation ($p < 0.01$), $n = 5$.

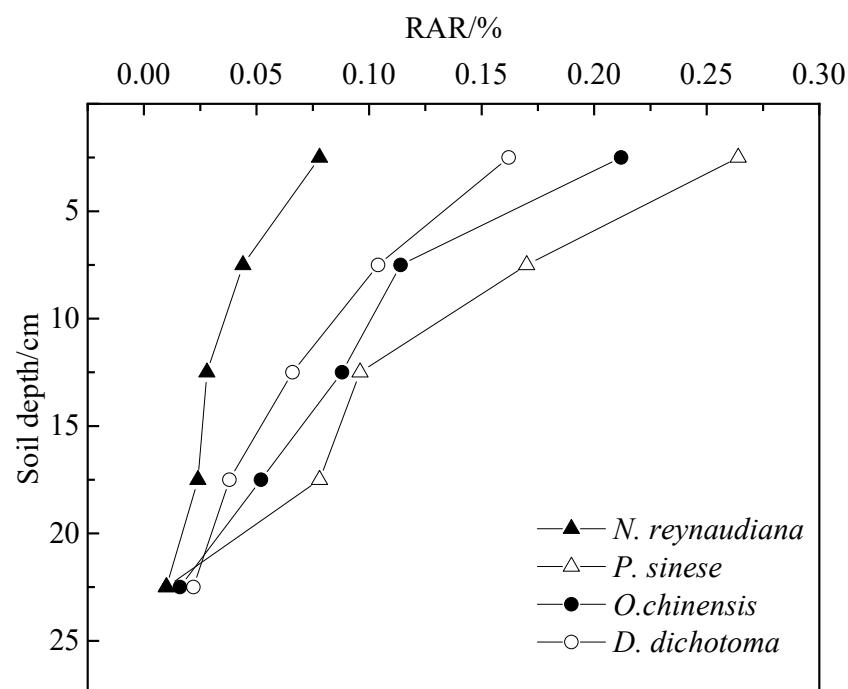
Table 10. The dominant factor equation of soil shear strength of different root–soil complexes (SS).

Vegetation Types	Dominant Factor Equation	R ²	n	NSE
<i>N. reynaudiana</i>	$SS = 101.11Rvd - 81.02L_{0.5-1} + 18.59$	0.99 **	5	0.99
<i>P. sinese</i>	$SS = 10.33Rld + 8.18$	0.99 **	5	0.99
<i>O. chinensis</i>	$SS = 25.18Rbd + 10.96$	0.99 **	5	0.99
<i>D. dichotoma</i>	$SS = 98.43Rvd + 4.87Smc - 117.06$	0.99 **	5	0.99
comprehensive	$SS = 31.61Rvd + 10.57$	0.89 **	20	0.89

Note: SS in the table is the shear strength of the soil shear strength of the root–soil complex. *Rld* is the root length density. *Rvd* is the root volume density. *Rbd* is the root biomass density. $L_{0.5-1}$ is the root with a root diameter of $0.5 < L \leq 1$ mm. *Smc* is soil moisture content. ** indicated extremely significant correlation ($p < 0.01$).

3.4. Correction of the WWM Model

The changes in the root RAR parameters of the four herbaceous plants with soil depth are shown in Figure 10. As seen from the figure, root RAR gradually decreases with increasing soil depth, and the maximum value existed in the 0–5 cm soil layer.

**Figure 10.** Changes of root RAR of the four herbaceous plants with soil depth.

The shear strength enhancement value obtained via actual measurements, the shear strength enhancement value determined via calculations and simulations, and the correction coefficient (k') are provided in Table 11. The table indicates that except for the four soil layers of 5–10 cm, 10–15 cm, 15–20 cm, and 20–25 cm, the predicted values obtained with the WWM model underestimated the measured increase in shear strength. The correction coefficient k' for each soil layer under the different vegetation conditions varied between 0.20 and 20.25. The average correction coefficient k' for *Neyraudia reynaudiana* was 0.88, that for *Pennisetum sinese* was 4.15, that for *Odontosoria chinensis* was 9.74, and that for *Dicranopteris dichotoma* was 5.00. The average correction coefficient k' of the WWM model with four species of vegetation was 4.94.

Table 11. Simulation and modification results of WWM model under different vegetation types.

Vegetation Types	Soil Depth (cm)	RAR /%	Average Tensile Strength /Mpa	Measured Shear Strength of Root–Soil Complex /kPa	Shear Strength of Bare Land /kPa	Measured Shear Strength Enhancement Value /kPa	Simulated Shear Strength Enhancement Value /kPa	Measured/Simulated (k')
<i>N. reynaudiana</i>	0–5 cm	0.078	51.29	28.21	17.10	11.11	4.80	2.31
	5–10 cm	0.044	54.96	15.12	12.47	2.66	2.90	0.92
	10–15 cm	0.028	61.79	11.35	10.94	0.42	2.08	0.20
	15–20 cm	0.024	63.10	10.50	9.95	0.55	1.82	0.30
	20–25 cm	0.010	74.76	9.79	9.19	0.60	0.90	0.67
<i>P. sinense</i>	0–5 cm	0.264	45.63	49.87	17.10	32.77	14.46	2.27
	5–10 cm	0.170	51.88	34.38	12.47	21.92	10.58	2.07
	10–15 cm	0.096	57.20	30.10	10.94	19.16	6.59	2.91
	15–20 cm	0.078	53.97	21.22	9.95	11.26	5.05	2.23
	20–25 cm	0.010	73.92	19.21	9.19	10.02	0.89	11.30
<i>O. chinensis</i>	0–5 cm	0.212	24.51	42.48	17.10	25.37	6.23	4.07
	5–10 cm	0.114	20.52	36.18	12.47	23.71	2.81	8.45
	10–15 cm	0.088	18.68	27.73	10.94	16.80	1.97	8.52
	15–20 cm	0.052	19.22	18.85	9.95	8.90	1.20	7.42
	20–25 cm	0.016	15.33	15.15	9.19	5.96	0.29	20.25
<i>D. dichotoma</i>	0–5 cm	0.162	16.80	40.46	17.10	23.36	3.27	7.15
	5–10 cm	0.104	21.40	21.51	12.47	9.04	2.67	3.38
	10–15 cm	0.066	29.66	19.68	10.94	8.75	2.35	3.72
	15–20 cm	0.038	17.23	14.44	9.95	4.48	0.79	5.71
	20–25 cm	0.022	51.29	10.12	9.19	0.93	0.18	5.05
Average	<i>N. reynaudiana</i>	0.037	61.35	14.99	11.93	3.06	2.71	1.13
	<i>P. sinense</i>	0.124	56.52	30.95	11.93	19.02	8.38	2.27
	<i>O. chinensis</i>	0.096	19.65	28.08	11.93	16.15	2.27	7.10
	<i>D. dichotoma</i>	0.078	18.42	21.24	11.93	9.31	1.73	5.37

4. Discussion

4.1. Effects of Four Herbaceous Plants on the Soil and Root Properties

Our study showed that the moisture content with vegetation was higher than that in bare land because vegetation roots can absorb and retain water [43]. The soil moisture content gradually increased with the increasing soil layer because of the strong permeability of the surface soil, the ease with which water penetrates from the surface to deeper layers, and the rapid evaporation of the surface soil water, all of which lead to lower water content in the surface soil than in the bottom layer [44–47]. In addition, the soil bulk density with vegetation was lower than that of bare soil because root entwining increased the soil porosity, thus reducing the bulk density [43,48]. The bulk density of the four vegetation species showed an overall increasing trend with increasing soil depth because the root content decreased with increasing soil depth. All root parameters of the four plants were greatest in the 0–5 cm surface layer, indicating that the roots were mainly concentrated in the surface soil. This is referred to as the surface aggregation phenomenon [49,50]. Additionally, the root parameters of the four plant species were significantly different, and the root parameters showed different downwards trends with increasing soil depth, which was related to the characteristics of the plants themselves. These results are consistent with the findings of Claus and George [51], Page and Gerwitz [52], and Yuan et al. [53] in the study of root distribution characteristics.

Previous studies demonstrated that the root tensile strength is related to the chemical composition and microstructure [54]. Table 3 indicates that the hemicellulose of *Neyraudia reynaudiana* and *Pennisetum sinense* was higher than that of *Odontosoria chinensis* and *Dicranopteris dichotoma*, resulting in a higher tensile strength in this paper. This is consistent with the research results of Hathaway and Penny [55], who researched the tensile characteristics of the roots of *Populus* and *Salix*, and Zhang et al. [56], who studied the role of the *Pinus tabulaeformis* root system in slope stabilization. Table 3 also reveals that the greater thickness

of the pericycle of *Neyraudia reynaudiana* and *Pennisetum sinense* could explain the higher tensile strength.

4.2. Effects of Four Herbaceous Species on the Shear Strength of the Root–Soil Complexes

The study results demonstrated that roots of different vegetation species have different enhancement effects on soil shear strength, which is caused by the distinct growth characteristics and structures of the different vegetation roots and varying bonding effects between roots and soil [57]. This finding is similar to the results obtained by Mahannopkul and Jotisankasa [25], who explored the shear strength of *Chrysopogon zizanioides* root–soil complexes and Bischetti et al. [54], who assessed the effects of the roots of various species, such as *Alnus viridis* and *Corylus avellana*, on soil stability. The shear strength of the root–soil complexes sharply decreased with the increasing soil depth according to different fitting equations. This pattern is related to the decrease in root configuration parameters. With the decrease in root parameters, the contact surface between the root and soil is reduced, and the combined effect of the two is weakened, which fails to give full play to the shear properties of the root, resulting in a decrease in the shear strength of the root–soil complex [37,58]. Due to the differences in plant root characteristics and parameters, there were differences between the fitting equations of the root–soil complexes of the different species with soil depth.

The addition of roots could significantly improve the shear strength of soil as shown in Table 8. The more roots there are, the greater the contact surface with the soil, the higher the cohesion between the roots and soil, and the higher the shear strength. In contrast, when root–soil complexes are loaded, the elasticity modulus of the roots is higher than that of the soil, which leads to relative displacement and frictional forces of the roots in the soil, and friction can transform external shear stress into internal root tensile forces, partly counteracting shear deformation and increasing the shear strength of the root–soil complexes [27,59]. At the same time, there was a significant positive correlation between the soil shear strength and roots with a root diameter (L) of $L \leq 0.5$ mm and $0.5 < L \leq 1$ mm, but there was no significant correlation with roots exhibiting a root diameter of $1 < L \leq 1.5$ mm and $L > 1.5$ mm, indicating that fine roots with a root diameter of $L \leq 1$ mm contributed more to shear strength enhancement. This occurs because under a high content of fine roots, roots play a major role in soil netting, shallow soil strengthening, and stability improvement [12,25,60,61]. Wu [26] studied the influence of vegetation on slope stability, Miller and Jastrow [62] explored soil structure stability, and Genet et al. [63] examined the characteristics of roots and obtained similar results. There is no significant negative correlation between the shear strength and tensile strength. The reason is that tensile strength is measured for single roots, while shear strength is measured for clusters.

The results obtained in this paper show that the shear strength of the root–soil complex is inversely proportional to the soil bulk density. This is contrary to the results obtained by Wei et al. [64] in their study of the effect of the bulk density on the soil shear strength and the results obtained by Ye et al. [65] in their research of the impact of the bulk density on soil characteristics. Generally, the higher the bulk density is, the closer the soil particles are and the higher the soil shear strength. However, in this experiment, the soil bulk density increased with the increasing soil layer depth, but the root content decreased, which reduced the strengthening effect of roots on the soil and caused a decline in the shear strength of root–soil complexes. In addition, there was a significant negative correlation between the shear strength of root–soil complexes and the soil moisture content in this experiment. This finding is similar to the results obtained by Huang et al. [9], who conducted an indoor test to explore the effect of *Neyraudia reynaudiana* roots on the shear strength of collapsing walls, and the results obtained by Fan and Su [66], who conducted an in situ shear test to study the soil fixation effect of moisture on the *Sesbania cannabina* root system. This effect occurred because with the increasing soil water content, the water film thickness increased, resulting in a decrease in the cohesive and binding forces among soil particles and between the roots and soil [9], causing a decrease in the shear strength of the root–soil complexes.

It is concluded that root length density, root surface area density, root volume density, root biomass density, roots with a root diameter of $L \leq 0.5$ mm, and roots with a root diameter of $0.5 < L \leq 1$ mm have an important positive effect on the shear strength of the root–soil complex, and root volume density has the greatest effect. In other words, with the increase in root volume, the bond between the root and soil becomes closer, and the mechanical properties of the root can better strengthen the soil and promote the shear strength of the soil. Mahannopkul and Jotisankasa [25] also noted that the shear strength of root–soil complexes increased with the increasing root content in their study of the shear strength of *Chrysopogon zizanioides* root–soil complexes. Bischetti et al. [67] suggested that the shear strength of *Fagus sylvatica*, *Picea abies*, and other root–soil complexes increased as a linear function of the root biomass. Ghestem et al. [68] studied *Ricinus communis*, *Jatropha curcas*, and *Rhus chinensis* and revealed that the root length and branch number of roots also significantly affected the mechanical properties of root–soil complexes. Therefore, the dominant factors of the shear strength of root–soil complexes differ among the different plant species.

4.3. Correction Coefficient of the WWM Model by the Pocket Vane Tester

In this test, the average correction coefficient of the WWM model by the pocket vane tester for each layer containing herbaceous roots ranged from 0.20 to 20.25, and the comprehensive average correction coefficient k' was 4.94. Nevertheless, some scholars have proposed that the correction coefficient should be below 0.56 for vegetation with small root diameters [21,28]. Schwarz et al. [69] observed, in an experiment quantifying the effect of vegetation roots on strengthening shallow landslides, that the WWM model correction coefficients for herb and tree roots ranged from 0.34 to 0.50. Fan and Su [70] experimentally evaluated the soil fixation effect of *Sesbania cannabina* roots and considered that the correction coefficient of the WWM model for this plant species varied between 0.39 and 0.42. Wu [71] also revised the model coefficient, proposing a correction coefficient of 0.25 when the root system was mainly shed without complete fracturing, while the coefficient should be reduced by 0.3–0.5 fold when the root system was partially shed or fractured. Different vegetation species exhibit distinct root growth characteristics and soil properties, leading to different correction coefficients of the WWM model.

Compared to the experimental results of other scholars, the correction coefficients in this study were relatively high, with all being greater than 1. This finding could be explained as follows: (1) in this experiment, the shear strength was measured with a 14.10 pocket vane tester. This vane tester more thoroughly cuts the root system inside the rotating blade so that the tensile characteristics of the root system can be more comprehensively manifested during measurement of the shear strength of root–soil complexes. However, when using an indoor direct shear instrument or direct shear box for shearing, the roots of the root–soil complex sample in the ring cutter could not all be cut off, and some roots could be pulled out [9,22,30,40,72]. The mechanical properties of the roots in the ring cutter are not fully developed, and the measured shear strength is low. (2) When measuring with a 14.10 pocket vane tester, the instrument was used to cut the root system via rotation. In this process, the vane tester not only fully manifested the shear characteristics of the root system but also entangled plant roots in the blades of the vane tester during instrument rotation, thus producing a pull effect on the instrument. Therefore, the shear tester needed to overcome the tensile effect of roots and the influence of winding and pulling in the shear process, leading to an increase in the measured shear strength value and correction coefficient k' of the WWM model. (3) In this study, undisturbed root–soil complexes were adopted, which preserved the bonds between the roots and soil and yielded a higher soil cohesion than that of remolded root–soil complexes, ultimately resulting in a higher shear strength of the undisturbed root–soil complexes [73]. Therefore, the WWM model correction coefficient was higher. However, the simulated shear strength enhancement values were less than the measured values because the correction coefficients k' were all less than 1 in the four soil layers of 5–10 cm, 10–15 cm, 15–20 cm, and 20–25 cm of *Neyraudia reynaudiana*. This

may be attributed to the high tensile strength of *Neyraudia reynaudiana* roots and that the pocket vane tester could not cut all the roots. Moreover, the RAR value of these four soil layers was low, which indicated that the root distribution of *Neyraudia reynaudiana* was low, and the winding effect of roots on the pocket vane tester was limited. The above aspects resulted in the pocket vane tester not fully manifesting the shear effect. In summary, the measured shear strength of the root–soil complexes of the Benggang collapsing wall was mostly higher than that obtained with the WWM model under field conditions. When the WWM model is modified under similar conditions, the correction coefficient determined in this test can be considered, and the average correction coefficient k' reaches 4.94.

5. Conclusions

With the increasing soil depth, the soil moisture content and bulk density increased, but the root length density, root surface area density, root volume density, and root biomass density of the four types of plants gradually decreased. The different root configuration parameters under the various vegetation conditions yielded distinct functional decline trends. The roots of each plant mainly included fine roots with root diameters (L) of $L \leq 0.5$ mm and $0.5 < L \leq 1$ mm. The average tensile strength of the four plants exhibited the order of *Neyraudia reynaudiana* > *Pennisetum sinense* > *Odontosoria chinensis* > *Dicranopteris dichotoma*. Plant roots combined with soil can significantly improve soil shear strength, and the average shear strength of the root–soil complexes of the four species followed the order *Pennisetum sinense* > *Odontosoria chinensis* > *Dicranopteris dichotoma* > *Neyraudia reynaudiana* > bare soil. These findings suggest that planting *Pennisetum sinense* has the best effects on increasing the shear strength of soil on Benggang in Southeast China. The enhancement effects of vegetation roots on the soil shear strength were largely concentrated in the 0–5 cm soil surface layer. With the increasing soil depth, the shear strength of the root–soil complexes decreased gradually. When exploring the dominant factor affecting the shear strength of root–soil complexes, the fitting results showed that root volume density exerted the greatest influence on the shear strength of root–soil complexes. Finally, the WWM model could be modified based on the shear strength of the root–soil complexes of *Neyraudia reynaudiana*, *Pennisetum sinense*, *Odontosoria chinensis*, and *Dicranopteris dichotoma*. The correction coefficient k' ranged from 0.20 to 20.25, and the average correction coefficient k' reached 4.94.

Author Contributions: Conceptualization, F.S., M.H., Y.H. and F.J.; data curation, F.S., M.H. and Y.H.; formal analysis, Y.Z. (Yue Zhang); funding acquisition, Y.Z. (Yue Zhang), Y.H. and F.J.; investigation, F.S., M.H., Y.Z. (Yuanyuan Zhan), Q.Z. and X.L.; methodology, F.S., Y.Z. (Yue Zhang), J.L. and F.J.; project administration, F.J.; resources, Y.H. and F.J.; software, F.S. and M.H.; supervision, F.S., Y.H. and F.J.; validation, F.J.; writing—original draft, F.S. and F.J.; writing—review and editing, F.S. and F.J. All authors have read and agreed to the published version of the manuscript.

Funding: Financial support for this study was provided by the National Natural Science Foundation of China (41977071), Water Conservancy Science and Technology Project of Fujian Province (No. KJg21009A), Forestry Peak Discipline Construction Project of Fujian Agriculture and Forestry University (72202200205).

Data Availability Statement: Not applicable.

Conflicts of Interest: The authors declare no conflict of interest.

References

1. Jiang, F.S.; Huang, Y.H.; Wang, M.K.; Lin, J.S.; Zhao, G.; Ge, H.L. Effects of Rainfall Intensity and Slope Gradient on Steep Colluvial Deposit Erosion in Southeast China. *Soil Sci. Soc. Am. J.* **2014**, *78*, 1741–1752. [[CrossRef](#)]
2. Lin, J.S.; Huang, Y.H.; Wang, M.K.; Jiang, F.S.; Zhang, X.B.; Ge, H.L. Assessing the sources of sediment transported in gully systems using a fingerprinting approach: An example from South-east China. *Catena* **2015**, *129*, 9–17. [[CrossRef](#)]
3. Zhang, L.T.; Sun, S.J.; Lin, M.Q.; Feng, K.J.; Zhang, Y.; Lin, J.S.; Ge, H.L.; Huang, Y.H.; Jiang, F.S. Study on soil-water characteristic curves in the profiles of collapsing walls of typical granite Benggang in southeast China. *PeerJ* **2022**, *10*, e13526. [[CrossRef](#)] [[PubMed](#)]

4. Chen, J.L.; Zhou, M.; Lin, J.S.; Jiang, F.S.; Huang, B.F.; Xu, T.T.; Wang, M.K.; Ge, H.L.; Huang, Y.H. Comparison of soil physicochemical properties and mineralogical compositions between noncollapsible soils and collapsed gullies. *Geoderma* **2018**, *317*, 56–66. [[CrossRef](#)]
5. Wei, Y.J.; Liu, Z.; Wu, X.L.; Zhang, Y.; Cui, T.T.; Cai, C.F.; Guo, Z.L.; Wang, J.G.; Cheng, D.B. Can Benggang be regarded as gully erosion? *Catena* **2021**, *207*, 105648. [[CrossRef](#)]
6. Okengwo, O.N.; Okeke, O.C.; Okereke, C.N.; Paschal, A.C. Geological and geotechnical studies of Gully Erosion at Ekwulobia, Oko and Nanka Towns, Southeastern Nigeria. *Electron. J. Geotech. Eng.* **2015**, *20*, 113–122.
7. Lin, J.H.; Huang, M.Y.; Zhang, L.T.; Chen, Y.; Shi, Y.Z.; Xu, Y.M.; Lin, J.S.; Huang, Y.H.; Jiang, F.S. Effect of root system of *Dicranopteris dichotoma* on soil shear strength of Benggang red soil layer. *J. Soil Water Conserv.* **2020**, *34*, 159–165, (In Chinese, with English abstract). [[CrossRef](#)]
8. Ajedegba, J.O.; Choi, J.W.; Jones, K.D. Analytical modeling of coastal dune erosion at South Padre Island: A consideration of the effects of vegetation roots and shear strength. *Ecol. Eng.* **2019**, *127*, 187–194. [[CrossRef](#)]
9. Huang, M.Y.; Sun, S.J.; Feng, K.J.; Lin, M.Q.; Shuai, F.; Zhang, Y.; Lin, J.S.; Ge, H.L.; Jiang, F.S.; Huang, Y.H. Effects of *Neyraudia reynaudiana* roots on the soil shear strength of collapsing wall in Benggang, southeast China. *Catena* **2022**, *210*, 105883. [[CrossRef](#)]
10. Ji, J.N.; Kokutse, N.; Genet, M.; Fourcaud, T.; Zhang, Z.Q. Effect of spatial variation of tree root characteristics on slope stability. A case study on Black Locust (*Robinia pseudoacacia*) and Arborvitae (*Platycladus orientalis*) stands on the Loess Plateau, China. *Catena* **2012**, *92*, 139–154. [[CrossRef](#)]
11. Leung, F.T.Y.; Yan, W.M.; Hau, B.C.H.; Thama, L.G. Root systems of native shrubs and trees in Hong Kong and their effects on enhancing slope stability. *Catena* **2015**, *125*, 102–110. [[CrossRef](#)]
12. Mattia, C.; Bischetti, G.B.; Gentile, F. Biotechnical characteristics of root systems of typical Mediterranean species. *Plant Soil* **2005**, *278*, 23–32. [[CrossRef](#)]
13. Abdi, E.; Majnouniana, B.; Genet, M.; Rahimi, H. Quantifying the effects of root reinforcement of Persian Ironwood (*Parrotia persica*) on slope stability; a case study: Hillslope of Hyrcanian forests, northern Iran. *Ecol. Eng.* **2010**, *36*, 1409–1416. [[CrossRef](#)]
14. Andreoli, A.; Chiaradia, E.A.; Cislighi, A.; Bischetti, G.B.; Comitia, F. Roots reinforcement by riparian trees in restored rivers. *Geomorphology* **2020**, *370*, 107389. [[CrossRef](#)]
15. Karimi, Z.; Abdi, E.; Deljouei, A.; Cislighi, A.; Shirvany, A.; Schwarz, M.; Halese, T.C. Vegetation-induced soil stabilization in coastal area: An example from a natural mangrove forest. *Catena* **2022**, *216*, 106410. [[CrossRef](#)]
16. Mao, Z.; Saint-André, L.; Genet, M.; Mine, F.X.; Jourdan, C.; Rey, H.; Courbaud, B.; Stokes, A. Engineering ecological protection against landslides in diverse mountain forests: Choosing cohesion models. *Ecol. Eng.* **2012**, *45*, 55–69. [[CrossRef](#)]
17. Hengchaovanich, D. VGT: A Bioengineering and Phytoremediation Option for the New Millennium. 2003. Available online: https://www.vetiver.org/PRVN_IVC2_35.PDF (accessed on 29 September 2022).
18. Loades, K.W.; Bengough, A.G.; Bransby, M.F.; Hallett, P.D. Planting density influence on fibrous root reinforcement of soils. *Ecol. Eng.* **2010**, *36*, 276–284. [[CrossRef](#)]
19. Abubakar, M. Contribution of Tea Root Reinforcement to Soil Shear Strength on Slope Stability. *J. Civ. Eng. Forum* **2018**, *4*, 13. [[CrossRef](#)]
20. Limon-Ortega, A.; Govaerts, B.; Sayre, K.D. Straw management, crop rotation, and nitrogen source effect on wheat grain yield and nitrogen use efficiency. *Eur. J. Agron.* **2008**, *29*, 21–28. [[CrossRef](#)]
21. Operstein, V.; Frydman, S. The influence of vegetation on soil strength. *Proc. ICE-Ground Improv.* **2000**, *4*, 81–89. [[CrossRef](#)]
22. Comino, E.; Druetta, A. The effect of Poaceae roots on the shear strength of soils in the Italian alpine environment. *Soil Tillage Res.* **2010**, *106*, 194–201. [[CrossRef](#)]
23. Xu, T.; Liu, C.Y.; Hu, X.S.; Xu, Z.W.; Shen, Z.Y.; Yu, D.M. Mechanical effect of vegetation slope protection under load in loess area of Xining Basin. *Trans. Chin. Soc. Agric. Eng.* **2021**, *37*, 142–151. [[CrossRef](#)]
24. Mokhammad, F.M. Shear strength of Apus bamboo root reinforced soil. *Ecol. Eng.* **2012**, *41*, 84–86. [[CrossRef](#)]
25. Mahannopkul, K.; Jotisankasa, A. Influences of root concentration and suction on *Chrysopogon zizanioides* reinforcement of soil. *Soils Found.* **2019**, *59*, 500–516. [[CrossRef](#)]
26. Wu, T.H.; Mckinnell III, W.P.; Swanston, D.N. Strength of tree roots and landslides on prince of Wales Island, Alaska. *Can. Geotech. J.* **1979**, *16*, 19–33. [[CrossRef](#)]
27. Waldron, L.J. The shear resistance of root-permeated homogeneous and stratified soil. *Soil Sci. Soc. Am. J.* **1977**, *41*, 843–849. [[CrossRef](#)]
28. Pollen, N.; Simon, A. Estimating the mechanical effects of riparian vegetation on stream bank stability using a fiber bundle model. *Water Resour. Res.* **2005**, *41*, 226–244. [[CrossRef](#)]
29. Schwarz, M.; Giadrossich, F.; Cohen, D. Modeling root reinforcement using a root-failure Weibull survival function. *Hydrol. Earth Syst. Sci.* **2013**, *17*, 4367–4377. [[CrossRef](#)]
30. Baets, S.D.; Poesen, J.; Reubens, B.; Wemans, K.; Baerdemaeker, J.D.; Muys, B. Root tensile strength and root distribution of typical Mediterranean plant species and their contribution to soil shear strength. *Plant Soil* **2008**, *305*, 207–226. [[CrossRef](#)]
31. Zhang, G.H.; Tang, M.K.; Zhang, X.C. Temporal variation in soil detachment under different land uses in the Loess Plateau of China. *Earth Surf. Processes Landf.* **2009**, *34*, 1302–1309. [[CrossRef](#)]
32. Wang, B.; Zhang, G.H.; Shi, Y.Y.; Zhang, X.C. Soil detachment by overland flow under different vegetation restoration models in the Loess Plateau of China. *Catena* **2013**, *116*, 51–59. [[CrossRef](#)]

33. Yu, Y.C.; Zhang, G.H.; Geng, R.; Sun, L. Temporal variation in soil detachment capacity by overland flow under four typical crops in the Loess Plateau of China. *Biosyst. Eng.* **2014**, *122*, 139–148. [[CrossRef](#)]
34. Wang, B.; Zhang, G.H.; Yang, Y.F.; Li, P.P.; Liu, J.X. The effects of varied soil properties induced by natural grassland succession on the process of soil detachment. *Catena* **2018**, *166*, 192–199. [[CrossRef](#)]
35. Yang, J.H.; Wang, C.L.; Dai, H.L. *Soil Agrochemical Analysis and Environmental Monitoring*; China Land Press: Beijing, China, 2008; (In Chinese, with English abstract)
36. Jackson, M.L. *Soil Chemical Analysis*, 2nd ed.; Jackson, M.L., Madison, W.I., Eds.; Prentice Hall, Inc.: Englewood Cliffs, NJ, USA, 1979.
37. Jiang, F.S.; He, K.W.; Lin, J.H.; Li, H.; Zhan, Z.Z.; Lin, J.S.; Ge, H.L.; Wang, M.K.; Huang, Y.H. A comparison of the effectiveness of the roots of two grass species in re-ducing soil erosion on alluvial fans in south-east China. *Hydrol. Process.* **2020**, *34*, 96–110. [[CrossRef](#)]
38. Soest, P.J.V. Using of detergents in the analysis of fibrous feeds. A rapid method for the determination of fibre and lignin. *J. Assoc. Off. Anal. Chem.* **1963**, *49*, 546–551.
39. Yuan, Z.L.; Xiong, S.P.; Li, C.M.; Ma, X.M. Effects of chronic stress of cadmium and lead on anatomical structure of tobacco roots. *Agric. Sci. China* **2011**, *10*, 1941–1948. [[CrossRef](#)]
40. Rossi, R.; Picuno, P.; Fagnano, M.; Amato, M. Soil reinforcement potential of culti-vated cardoon (*Cynara cardunculus* L.): First data of root tensile strength and density. *Catena* **2022**, *211*, 106016. [[CrossRef](#)]
41. Wang, D.H. *Multivariate Statistical Analysis and SPSS Application*, 2nd ed.; East China University of Science and Technology Press: Shanghai, China, 2018; (In Chinese, with English abstract).
42. Wu, T.H.; Beal, P.E.; Lan, C. In-situ shear test of soil-root systems. *Geotech. Eng.* **1988**, *114*, 1376–1394. [[CrossRef](#)]
43. Han, G.Z.; Zhang, G.L.; Gong, Z.T.; Wang, G.F. Pedotransfer functions for estimating soil bulk density in China. *Soil Sci.* **2012**, *177*, 158–164. [[CrossRef](#)]
44. Li, X.R.; Ma, F.Y.; Xiao, H.L.; Wang, X.P.; Kim, K.C. Long-term effects of revegetation on soil water content of sand dunes in arid region of Northern China. *J. Arid. Environ.* **2004**, *57*, 1–16. [[CrossRef](#)]
45. Na, R.S.; Du, H.B.; Na, L.; Shan, Y.; He, H.S.; Wu, Z.F.; Zong, S.W.; Yang, Y.; Huang, L.R. Spatiotemporal changes in the Aeolian desertification of Hulunbuir Grassland and its driving factors in China during 1980–2015. *Catena* **2019**, *182*, 104123. [[CrossRef](#)]
46. Zhao, Y.L.; Wang, Y.Q.; Wang, L.; Fu, Z.H.; Zhang, X.Y.; Cui, B.L. Soil-water stor-age to a depth of 5 m along a 500-km transect on the Chinese Loess Plateau. *Catena* **2017**, *150*, 71–78. [[CrossRef](#)]
47. Zhang, J.Y.; Duan, L.M.; Liu, T.X.; Chen, Z.X.; Wang, Y.X.; Li, M.Y.; Zhou, Y.J. Experimental analysis of soil moisture response to rainfall in a typical grassland hillslope under different vegetation treatments. *Environ. Res.* **2022**, *213*, 113608. [[CrossRef](#)] [[PubMed](#)]
48. Li, T.C.; Shao, M.A.; Jia, Y.H. Application of X-ray tomography to quantify macropore characteristics of loess soil under two perennial plants. *Eur. J. Soil Sci.* **2016**, *67*, 266–275. [[CrossRef](#)]
49. Hendrick, R.L.; Pregitzer, K.S. Temporal and Depth-Related Patterns of Fine Root Dynamics in Northern Hardwood Forests. *J. Ecol.* **1996**, *84*, 167–176. [[CrossRef](#)]
50. Bordron, B.; Robin, A.; Oliveira, I.R.; Guillemot, J.; Laclau, J.P.; Jourdan, C.; Nouvellon, Y.; Abreu-Junior, C.H.; Trivelin, P.C.O.; Gonçalves, J.L.M.; et al. Fertilization increases the functional specialization of fine roots in deep soil layers for young Eucalyptus grandis trees. *For. Ecol. Manag.* **2019**, *431*, 6–16. [[CrossRef](#)]
51. Claus, A.; George, E. Effect of stand age on fine-root biomass and biomass distribu-tion in three European forest chronosequences. *Can. J. For. Res.* **2005**, *35*, 1617–1625. [[CrossRef](#)]
52. Page, E.R.; Gerwitz, A. Mathematical models, based on diffusion equations, to de-scribe root systems of isolated plants, row crops, and swards. *Plant Soil* **1974**, *41*, 243–254. [[CrossRef](#)]
53. Yuan, H.X.; Gao, Z.L.; Zhang, X.; Du, J.; Zhang, X.J. Root distribution and tensile resistance characteristics of slope protection plants. *South North Water Divers. Water Sci. Technol.* **2016**, *14*, 117–123, (In Chinese, with English abstract). [[CrossRef](#)]
54. Bischetti, G.B.; Chiaradia, E.A.; Simonato, T.; Speziali, B.; Vitali, B.; Vullo, P.; Zocco, A. Root Strength and Root Area Ratio of Forest Species in Lombardy (Northern Italy). *Plant Soil* **2005**, *278*, 11–22. [[CrossRef](#)]
55. Hathaway, R.L.; Penny, D. Root Strength in Some Populus and Salix Clones. *N. Z. J. Bot.* **1975**, *13*, 333–344. [[CrossRef](#)]
56. Zhang, C.B.; Chen, L.H.; Jiang, J. Why fine tree roots are stronger than thicker roots: The role of cellulose and lignin in relation to slope stability. *Geomorphology* **2014**, *206*, 196–202. [[CrossRef](#)]
57. Zhang, C.B.; Chen, L.H.; Liu, Y.P.; Ji, X.D.; Liu, X.P. Triaxial compression test of soil-root composites to evaluate influence of roots on soil shear strength. *Ecol. Eng.* **2010**, *36*, 19–26. [[CrossRef](#)]
58. Prasad, R. A linear root water uptake model. *J. Hydrol.* **1988**, *99*, 297–306. [[CrossRef](#)]
59. Hu, X.S.; Brierley, G.; Zhu, H.L.; Li, G.R.; Fu, J.T.; Mao, X.Q.; Yu, Q.Q.; Qiao, N. An exploratory analysis of vegetation strategies to reduce shallow landslide activity on loess hillslopes, Northeast Qinghai-Tibet Plateau, China. *J. Mt. Sci.* **2013**, *10*, 668–686. [[CrossRef](#)]
60. Osman, N.; Barakbah, S.S. Parameters to predict slope stability—Soil water and root profiles. *Ecol. Eng.* **2006**, *28*, 90–95. [[CrossRef](#)]
61. Zhuang, L.Y.; Yang, W.Q.; Wu, F.Z.; Tan, B.; Zhang, L.; Yang, K.J.; He, R.Y.; Li, Z.J.; Xu, Z.F. Diameter-related variations in root decomposition of three common sub-alpine tree species in southwestern China. *Geoderma* **2018**, *311*, 1–8. [[CrossRef](#)]

62. Miller, R.M.; Jastrow, J.D. Hierarchy of root and mycorrhizal fungal interactions with soil aggregation. *Soil Biol. Biochem.* **1990**, *22*, 579–584. [[CrossRef](#)]
63. Genet, M.; Stokes, A.; Salin, F.; Mickovski, S.B.; Fourcaud, T.; Dumail, J.F.; Beek, R.V. The influence of cellulose content on tensile strength in tree roots. *Plant Soil* **2005**, *278*, 1–9. [[CrossRef](#)]
64. Wei, J.; Shi, B.L.; Li, J.L.; Li, S.S.; He, X.B. Shear strength of purple soil bunds under different soil water contents and dry densities: A case study in the Three Gorges Res-ervoir Area, China. *Catena* **2018**, *166*, 124–133. [[CrossRef](#)]
65. Ye, C.; Guo, Z.L.; Cai, C.F.; Wang, J.G.; Deng, J. Effect of water content, bulk den-sity, and aggregate size on mechanical characteristics of Aquults soil blocks and ag-gregates from subtropical China. *J. Soils Sediments* **2017**, *17*, 210–219. [[CrossRef](#)]
66. Fan, C.C.; Su, C.F. Role of roots in the shear strength of root-reinforced soils with high moisture content. *Ecol. Eng.* **2008**, *33*, 157–166. [[CrossRef](#)]
67. Bischetti, G.B.; Chiaradia, E.A.; Epis, T.; Morlotti, E. Root cohesion of forest species in the Italian Alps. *Plant Soil* **2009**, *324*, 71–89. [[CrossRef](#)]
68. Ghestem, M.; Veylon, G.; Bernard, A.; Vanel, Q.; Stokes, A. Influence of plant root system morphology and architectural traits on soil shear resistance. *Plant Soil* **2014**, *377*, 43–61. [[CrossRef](#)]
69. Schwarz, M.; Preti, F.; Giadrossich, F.; Lehmann, P.; Or, D. Quantifying the role of vegetation in slope stability: A case study in Tuscany (Italy). *Ecol. Eng.* **2010**, *36*, 285–291. [[CrossRef](#)]
70. Fan, C.C.; Su, C.F. Effect of soil moisture content on the deformation behaviour of root-reinforced soils subjected to shear. *Plant Soil* **2009**, *324*, 57–69. [[CrossRef](#)]
71. Wu, T.H. Root reinforcement of soil: Review of analytical models, test results, and ap-plications to design. *Can. Geotech. J.* **2013**, *50*, 259–274. [[CrossRef](#)]
72. Schwarz, M.; Cohen, D.; Or, D. Root-soil mechanical interactions during pullout and failure of root bundles. *J. Geophys. Res.* **2010**, *115*, F04035. [[CrossRef](#)]
73. Zhu, J.Q.; Su, B.R.; Wang, Y.Q.; Wang, Y.J.; Li, Y.X. Changes of soil fixation func-tion of thorns root system with soil moisture content. *For. Sci.* **2020**, *56*, 202–208, (In Chinese, with English abstract). [[CrossRef](#)]